

~~66-10-82~~
MU8-15

RECONNAISSANCE GEOLOGY AND GEOLOGIC HAZARDS
OF SELECTED AREAS OF THE SOUTHERN
CALIFORNIA CONTINENTAL BORDERLAND CONSIDERED
FOR OCS PETROLEUM LEASE SALE 48

by OFFICE 001

Clarke, S. H., Greene, H. G., Field, M. E.,
Lee, W. H. K., and McCrory, P. A.

July, 1982

CONTENTS

	Page
Introduction -----	1
Geographic and Geological Setting -----	1
Previous Investigations -----	2
Acknowledgements -----	3
Procedures and Methods -----	3
Methods of Interpretation -----	4
Gulf of Santa Catalina and Adjacent Shelf -----	6
Introduction -----	6
Geologic Structure -----	9
Seismicity -----	12
Tsunamis -----	15
Seafloor Instability -----	16
Hydrocarbon Seepage and Shallow Gas Accumulations -----	21
Sediment Thickness and Character -----	23
Summary of Hazards -----	26
Central Santa Rosa-Cortes Ridge -----	28
Introduction -----	28
Geologic Structure -----	30
Seismic Hazards -----	32
Seafloor Instability -----	34
Hydrocarbon Seepage and Shallow Gas Accumulations -----	36
Sediment Character and Thickness -----	36
Summary of Hazards -----	38
Western Santa Barbara Channel - Point Conception Region -----	39
Introduction -----	39
Seismic Interpretations -----	42

CONTENTS, cont' d.

Geologic Structure -----	47
Seismicity -----	51
Seafloor Instability -----	54
Hydrocarbon Seepage and Shallow Gas Accumulations -----	57
Bedrock Geology -----	57
Summary of Hazards -----	58
References Cited -----	60
Appendix 1. Location, Depth, Length and	
Type of Selected Samples from the	
Southern California Continental	
Borderland -----	68
List of Figures	
1. Location Map, Gulf of Santa Catalina	
and Adjacent Area -----	7
2. Location Map, Central Santa Rosa -	
Cortes Ridge Area -----	29
3. Location Map, Western Santa Barbara	
Channel - Point Conception Area -----	40
4. Interpreted Seismic Reflection Profile	
(line 131, S2-78SC) -----	43
5. Interpreted Seismic Reflection Profile	
(line 114, S2-78SC) -----	44

LIST OF PLATES

- Plate 1. Index map of continental borderland of southern California showing tracts recommended for proposed lease sale.
- 2* Geophysical **trackline** map of the Gulf of Santa Catalina **area**.
- 3* Sample locations and ages, Gulf of Santa Catalina area, California
- 4* **Fault** and Seismicity map of the Santa Catalina area.
- 5* **Surficial** geologic map of the Gulf of Santa Catalina and adjacent area, California.
6. **Isopach** map of inferred Quaternary sediments in the Gulf of Santa Catalina area, California.
7. Geophysical trackline map of the San **Nicolas** Island area.
8. Bedrock geology of the central Santa Rosa-Cortes Ridge (from Vedder and others, 1974).
9. Preliminary structure map central Santa **Rosa-Cortes** Ridge.
10. Earthquake epicenters Jan. 1, 1932 to Sept. 30, 1979, central Santa **Rosa-Cortes** Ridge.
11. Seafloor instability, erosion and transport, central Santa **Rosa-Cortes** Ridge.
12. Offshore **surficial** geology, central Santa **Rosa-Cortes** Ridge.
13. Grain-size and percent calcium carbonate and organic carbon in surface sediments central Santa **Rosa-Cortes** Ridge.
14. Geophysical **trackline** map of the Point Conception area.
15. Geologic map of the Point Conception area, California.
16. **Surficial** geologic and morphologic map of the Point Conception area, California.
17. **Isopach** map of inferred Quaternary sediment in the Point Conception area, California.
18. Fault and seismicity map of the Point Conception area, California.

RECONNAISSANCE GEOLOGY AND GEOLOGIC HAZARDS OF SELECTED
AREAS OF THE SOUTHERN CALIFORNIA CONTINENTAL BORDERLAND
CONSIDERED FOR OCS PETROLEUM LEASE SALE 48

INTRODUCTION

Accelerated exploration and exploitation of hydrocarbons in the southern California continental borderland have necessitated the consideration of potential geoenvironmental hazards in the vicinity of lease tracts. This report addresses geological hazards present in and around some lease sale blocks that were initially considered for inclusion in **OCS** lease sale #48. Three areas were studied, the Gulf of Santa Catalina, the northern part of the **santa Rosa-Cortes** Ridge, and the westernmost Santa Barbara Channel just offshore from Point Conception (pi. 1). These are significant because they lie in close proximity to highly populated urban centers, (2) near sites or potential sites of critical industries onshore, or (3) adjoin or overlap areas previously surveyed by the U.S. Geological Survey (USGS) in its geological environmental appraisal for lease sale #35. Geological environmental assessments undertaken in other parts of the southern California borderland by the USGS in conjunction with offshore leasing activities are reported by Greene and others (1975).

Geographic and Geological Setting

The term southern California continental borderland here refers to the region extending from the Channel Islands (San Miguel, Santa Rosa, **Santa Cruz,** and **Anacapa** Islands) on the north to the U.S.-Mexican border on the south and from the California coastline, westward approximately 250 **km** to the Patton Escarpment (pi. 1). This report is concerned with the environmental geology **of** parts of three areas within the borderland that include most of the tracts proposed for leasing **in** OCS sale 48. The geologic framework of the southern

California continental borderland is described in recent studies by Vedder and others (1974; 1980).

Previous Investigations

Since 1975, the USGS has studied the geological environment of the southern California continental borderland and assessed, on a regional scale, geologic hazards pertinent to petroleum development on the OCS. Although much geologic and oceanographic work was done in this region prior to 1975, few of these studies were directed at environmental geologic problems. Some significant investigations that focus on geological hazards are noted below.

The first thorough investigation of onshore and offshore faulting in southern California was carried out by Gutenberg (1943); a study of offshore seismic events by **Clements** and Emery (1947) provided additional details concerning the regional geologic structure. D. G. Moore's (1960) study of the shear strength and **depositional** patterns of sediments in the borderland gave indications as to how the region would react to active faulting. Known and postulated faults, both offshore and onshore, have been compiled by Jennings (1973, 1977). A geologic reconstruction of part of the borderland by Howell and others (1974) implies that strike-slip faulting is dominant. Evaluation of seismic activity in the borderland led Vedder and others (1974) to the conclusion that fault location and movement may be much more complex than was thought by earlier workers. Recent detailed studies of faulting in selected areas of the borderland indeed indicate that the pattern of faulting is complex and appears to result from wrench-fault tectonics (Greene and others, 1975; 1979; Yerkes and others, 1980).

In their study of the origin of petroleum, Emery and **Rittenberg** (1952) examined sediments from twelve borderland basins to determine their

composition, age and method of deposition, and the presence **of** hydrocarbons. Orr and Emery (1956) contributed additional knowledge concerning the origin and distribution of hydrocarbons in borderland basins. Emery and **Hoggan** (1958) discussed the types of gases occurring in oil-bearing regions, and compared them to types found in several borderland basins. Naturally occurring oil and gas seeps in the southern California offshore region were described **by** Wilkinson (1971). **Mikolaj** and others (1972) subsequently extended and refined this **work** in their study of offshore oil seeps.

Acknowledgements

Many colleagues in the USGS have helped collect and interpret data used in this report; special thanks to Robert **Arnal**, Paula **Quinterno**, Keith **Kvenvolden**, John Vedder, Kimberly Bailey, William Richmond, Carol Hirozawa, Kevin Heston, Michael White, and to Michael Kennedy of the California Division of Mines and Geology. Our thanks also go to Mary Jane Kibbee, who typed the manuscript. Collection and interpretation of marine geological and geophysical data for this study was funded in part by the Bureau of Land Management (**BIM**) under the **BIM-USGS** Memorandum of Understanding (**MOU**) **AA551-MUS-15**.

Procedures and Methods

Much of the material presented in this report is based on the interpretation of seismic reflection records collected aboard the R/V SEA SOUNDER during 1978 and 1979 (cruises **S2-78SC** and **S2-79SC**). Both **high-resolution** profiles gathered with 3.5 kHz and **Uniboam** systems and intermediate to deep-penetration profiles gathered with a 160 **kJ** sparker system were used. Subsurface features ranging upward in size from approximately 0.3 m to

1.5 m could be resolved on high resolution reflection records that varied in **subbottom** penetration from 150 m to over 400 m. The deep-penetration records used to determine deep structure can resolve features larger than about 15 m in size and commonly record geologic structure at depths of **well** over a kilometer in deep sedimentary basins. Ship positioning employed a range-range MiniRanger system during approximately 80 percent of time; this system was augmented or replaced by ship's radar during the remainder of these cruises. Location accuracy of the seismic data ranges from about 15 m, to about 500 m where ship's radar alone was used.

Methods of Interpretation

Standard interpretive methods were used in the **analysis** of the seismic reflection data. For a description of basic seismic reflection techniques, the interested reader is referred to Moore (1960) and Payton (1977). Criteria for the interpretation of faults are as follows (after Greene and others, 1973) : Well defined faults: (1) distinct displacement of prominent reflectors, (2) a sharp discontinuation of prominent reflectors, or the juxtaposition of prominent reflectors with an interval having contrasting seismic characteristics, or (3) an abrupt change in the dips of reflectors across a distinct boundary. Inferred faults: (1) small displacement of prominent reflectors, in which the upper or shallow reflectors may be bent rather than broken, (2) prominent reflectors are discontinuous and contrasting seismic characteristics are present on either side of an obscure, seismically disturbed zone, **or** (3) apparent changes in dip on either side of the seismically disturbed zone. Questionable faults are mapped where obscure interruptions of seismic reflectors occur in the subsurface. Such interruptions consist of (1) a shift in phase of reflectors that is not due to

instrumental malfunction, (2) bent or broken reflectors that can be correlated with known faults on other lines, (3) discontinuation of weak reflectors, or (4) any other zone of seismic contrast, especially where the zone appears similar to and aligned with faults identified on adjacent lines. Some questionable and inferred faults have been mapped where anomalous topographic **lineaments** appear to support the continuation of known faults. Slump **scarps** are mapped on the basis of the characteristics described above and on other criteria such as sharply defined, steeply dipping slopes associated with the **hummocky** surfaces and contorted stratification thought to indicate slump deposits.

The orientation of faults is determined principally by correlation from one seismic line to another. Faults are correlated between adjacent lines mainly on the basis of their association with similar structural and seismic features on adjacent profiles. Such features typically include reflectors which are similar and are displaced in the same direction, with similar drag or other subsidiary folding, and contrasts in seismic characteristics across a fault that are similar on adjacent lines. Faults that cannot be correlated from one line to the next are drawn parallel to nearby (within about 2 km) faults that have been correlated between **two** or more adjacent lines.

Where fault planes dip more than about 35°, the vertical exaggeration common to seismic records precludes determining the dip even though the records clearly indicate that a fault is present. Consequently, faults dipping 35° or more are drawn as vertical. Determination of the amount and direction of movement on a fault is very difficult. Only the apparent vertical **component** (vertical separation) of offset can be measured on the seismic reflection profiles; the horizontal component (strike-slip separation) is almost impossible to determine.

The upper limit of a fault can be calculated from seismic records by multiplying the assumed velocity through the sediments by half of the two-way seismic travel time obtained at the shallowest (**stratigraphically** highest and youngest) subsurface reflector cut by the fault. Generally the **stratigraphically** highest point at which a fault can be identified in a seismic reflection profile is at the base of the "bubble pulse"^{1/}, about 6 m beneath the ocean floor in **high-resolution** records and about 60 m below the floor in intermediate-penetration records. An exception is where the sea floor is actually displaced by the fault.

GULF OF SANTA CATALINA AND ADJACENT SHELF

Introduction

This area comprises the offshore region extending from the latitude of Long Beach southward to that of San **Diego**, and from the shoreline seaward an average distance of about 36 km (fig. 1). The mainland shelf is the major **physiographic** feature in the eastern part of the study area. It may be subdivided, for convenience? into three parts: a relatively broad (10-20 km wide) segment, here referred to as the San Pedro shelf, between the Pales Verdes Hills and Newport Beach, a narrow (3-9 km wide) segment between Newport Beach and Point La Jolla, and a relatively wide (~ 7-17 km wide) segment, here referred to as the San **Diego** shelf, between Point La Jolla and the U.S.-
a Mexican border. The break in slope marking the shelf **edge** is as shallow as

^{1/} A bubble-pulse consists of attenuating reverberations that linger in the water column after the primary pulse has been produced. These reverberations are reflected back from the ocean bottom and appear as **psuedo-sea-floor** traces on the seismic record, effectively masking any signals reflected from shallow structures immediately beneath the sea floor.

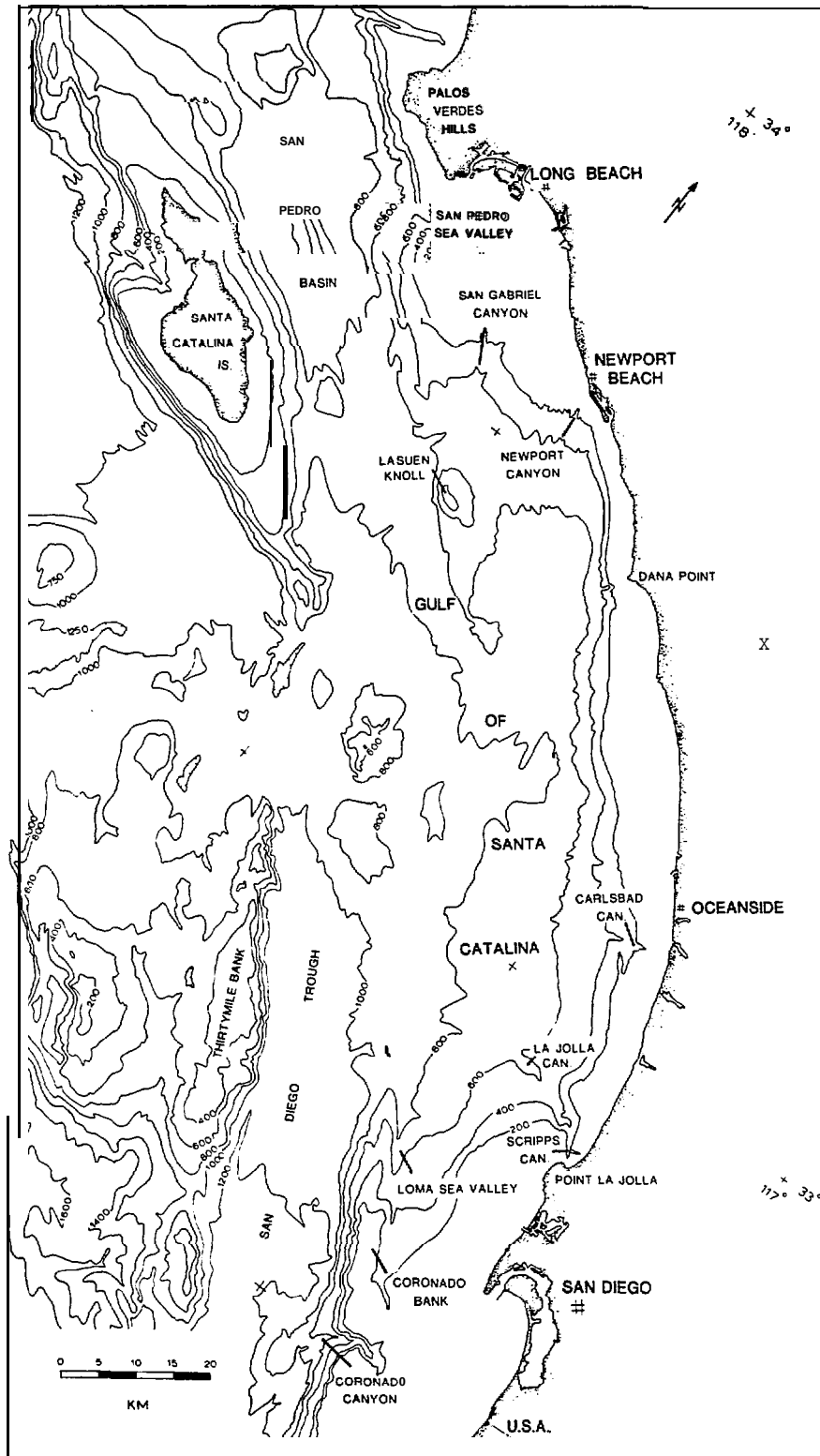


Figure 1. Location map, Gulf of Santa Catalina and adjacent area.

4

75 m in the northern part of the area off the Pales Verdes Hills and locally along the San Pedro shelf, but characteristically occurs within the depth range from about 90 m to 125 m over the remainder of this region. Water depths over the entire area studied range from approximately 20-30 m along the inner shelves to a maximum of about 1250 m in the San Diego Trough west of Coronado **Bank**.

Prominent submarine canyons cutting the San Pedro shelf include the San Pedro Sea Valley, **which** empties westward into the San Pedro Basin, and the San Gabriel and Newport Canyon systems, which cut the southern margin of the shelf and drain southward into the Gulf of Santa Catalina. The latter canyon system forms the **physiographic** boundary between the San Pedro shelf and the narrow shelf segment south of Newport Beach. **Carlsbad** Canyon heads on the inner shelf approximately 7 km south of Oceanside and extends westward into the Gulf of Santa Catalina. Farther south, La Jolla Canyon and its tributary, Scripps Canyon, cut the shelf north of Point La Jolla, forming the northern boundary of the San Diego shelf segment. They then flow westward into the Gulf of Santa Catalina. The mainland shelf off San Diego **is** cut by a major **northwest-**trending valley, Loma Sea Valley. To the west lies a northwest-trending submarine basement ridge, Coronado **Bank**, that rises to depths as shallow as 97 m. Coronado Canyon heads on the outer shelf about 25 **km** southwest of San Diego and empties southwestward into the San Diego Trough, delimiting Coronado Bank on the south.

The Gulf of Santa Catalina is bounded on the west by prominent bedrock ridges comprising the emergent Santa Catalina Island platform and **Thirtymile** Bank, which rises over 850 m above the floor of the adjacent San Diego Trough. Several prominent bedrock knolls, e.g., Lasuen Knoll, rise as much as 420 m above the sea floor in the northern half of the Gulf of **Santa** Catalina.

Data used in this study **were** collected during the May-June, 1978 cruise of the R/V SEA SOUNDER (**S2-78-SC; pl. 2**). A preliminary map depicting the overall geologic structure of this area was prepared from **intermediate-** penetration, low-resolution single channel sparker data. Subsequently, shallow-penetration, high-resolution **boomer** and sparker records were used to prepare maps showing shallow structure and faults, bedrock outcrops, areas of active sediment transport and potential seafloor instability, hydrocarbon seeps and gas anomalies, and unconsolidated sediment distribution and thickness. Geophysical data collected during the 1979 cruise of the R/V SEA SOUNDER (**S2-79-SC; pl. 2**) were used to fill data voids and **to** aid in the correlation of major structures and geologic contacts. Forty-five dart and gravity cores collected during the 1978 cruise and selected samples from the 1979 cruise **were** used to provide geologic age information for interpretation of geophysical records, and a limited amount of textural date (pi. 3). Core **type**, location, water depth and recovery results at each sampling station are listed in Appendix 1.

Geologic Structure

The predomimnt structural grain within the Gulf of Santa Catalina and San Diego Trough has a northwest trend (pi. 4). **Two** major fault zones within these areas bound a relatively undeformed structural block, named the Catalina block by Greene and others [1979). The **Newport-Inglewood-Rose** Canyon fault zone forms the northeast boundary of this block, and the Pales Verdes **Hills-Coronado** Bank fault zone forms the southwest boundary. Both of these fault zones are **composed** of discontinuous, generally right-stepping, en-echelon faults and associated folds (pi. 4). No single fault within either zone appears to continue uninterrupted for more than 40 km. This pattern resembles

other fault zones of California, onshore and offshore, which are **composed** of **short**, en-echelon faults in relatively narrow (**1** to 10 km wide) zones.

The Newport-Inglewood-Rose Canyon fault zone, which extends offshore at Newport Beach, appears to have influenced the development of the eastern slope of the Gulf of Santa Catalina **physiographic** basin. The zone **is** defined at the surface by discontinuous, generally northwest-trending faults and folds within Tertiary and Quaternary strata (pi. 4); these structural features form a discrete belt that extends for at least 240 km from near the Santa Monica Mountains into Baja California. To the south, near Oceanside, the faults of this zone step to the west and continue southward to La Jolla. Continuation of this fault zone is proposed by Legg and Kennedy (1979), who connect the Rose Canyon fault zone with the **Vallecitos-San Miguel** fault zone in Mexico. Onshore and northwest of Newport Beach, the fault zone extends northward across the western Los Angeles Basin and appears to terminate abruptly at the Santa Monica fault (Barrows, 1974; Ziony and others, 1974; Jennings, 1977). Moody and Hill (1956) and Harding (1973) postulate a right-slip wrench tectonic model for the **Newport-Inglewood** fault zone in the Los Angeles Basin. Features suggesting this same sense of motion have been noted by us offshore along the southern extension of the zone, e.g. , Scripps submarine canyon appears to be a right-laterally offset head of La Jolla submarine canyon. The inner, north-trending segment of La Jolla canyon also is **fault-**controlled; it probably was formed by erosion along a shear zone created by motion along the Rose Canyon fault.

The Pales Verdes Hills-Coronado Bank fault zone extends from Santa Monica to Loma Sea Valley and beyond (pi. 4). The segment of the fault zone near San Pedro forms the **western** margin of the Catalina block; here, it is well defined and continuous. Farther south it is discontinuous along the eastern edge of

Lasuen Knoll; however, a strand of the fault zone steps westward, extending along the western edge of Lasuen Knoll. The Pales Verdes Hills-Coronado Bank fault zone may **be** traced southward for 30 km **or** more to its intersection with a more north-trending fault about 25 km west of Point La Jolla. From this intersection, the Pales Verdes Hills-Coronado Bank **fault** zone continues southward as two parallel strands along the eastern edge of Coronado **Bank**. This fault zone is shown **by** Legg and Kennedy (1979) to continue south into Mexico, where it connects with the Agua **Blanca** fault zone. We suggest that the Pales Verdes **Hills-Coronado Bank** fault zone has exerted structural control on the development of Loma Sea Valley and the eastern slope of Coronado Bank during Quaternary time.

Another, shorter fault is mapped in the central part of the San Diego Trough (pi. 4). Legg and Kennedy (1979) have proposed that this fault joins the San Pedro and Santa Catalina faults to the north, and the **Thirtymile** Bank and Maximinos faults to the south. If so, this fault zone is as long as those bounding the Catalina block and probably developed in a similar manner. This suggests the presence in the southern part of the study area of another structural block that is bounded on the east by the Pales Verdes **Hills-Coronado Bank** fault zone and on the west by the San Pedro-San Diego Trough-**Maximinos** fault zone.

The length, trend, and character of the three major offshore fault zones described above are comparable to the Whittier-Elsinore and San Jacinto fault zones onshore. Short, en-echelon, second-order faults are associated with each major fault zone and commonly splay from the primary faults at angles ranging from 20 to 40 degrees. Second-order fold axes are similarly related to these fault zones. These structural relationships follow the stress pattern for wrench faulting described by Moody and Hill (1956) and Wilcox and

others (1973), and suggest that the offshore fault zones may represent through-going, right-slip faults within the underlying basement rocks.

Major structural and **physiographic** features within and bounding the **Catalina** block are compatible with the wrench tectonic model. We suggest that La Jolla Submarine Canyon, for example, is a graben formed as a result of tension associated with dilation within the Catalina block. Similarly, Coronado Bank, Point **Loma**, and other banks and ridges within and adjacent to the Catalina block appear to be horsts produced by compression. This horst and graben topography and the buried sedimentary basins and ridges in the San Diego region may also express a structural history dominated by wrench tectonics (Michael P. Kennedy, oral communication, 1978).

Seismicity

The Gulf of Santa Catalina region has been seismically active throughout historic time, especially the northwestern part of the area in the vicinity of the San Pedro shelf and Pales Verdes Hills. The distribution of instrumentally recorded earthquakes is shown on Plate 4; the locations of these epicenters were provided by **W.H.K.** Lee from instrumental data collected by the southern California seismographic network, established in 1926 and now **comprising** 160 stations operated under the joint direction of the Seismological Laboratory of the California Institute of Technology and the U.S. Geological Survey. Location accuracy of epicenters offshore is estimated to be approximately 5 **km (W.H.K. Lee, 1980, personal commun.)**.

Non-instrumentally recorded (felt) earthquakes in this region are cataloged by **Townley** and Allen (1939). The locations of most earthquakes recorded by the southern California network during the 40-year period between 1932 and 1972 have been compiled on a yearly basis by **Hileman** and others

(1973); epicenter locations for 1973-1974 are reported by Friedman and others (1976) . In addition, an earthquake data file compiled from the California Institute of Technology and other sources for seismic events reported between 1900 and 1977 is maintained by the California Division of Mines and Geology (Real and others, 1978).

Epicenters located by the southern California network within the Gulf of Santa Catalina region between January, 1932 and September, 1979 show a random pattern, generally lacking clear associations with major faults or other structures (pi. 4). More than 400 shocks measuring M2 to M4 are plotted in the offshore area and over 200 are plotted in the onshore coastal area. Earthquakes measuring between M4 and M6 are recorded at more than 30 offshore locations and at over 25 onshore coastal locations. The larger events appear to be concentrated in the Pales Verdes Hills area, and many lie in the vicinity of the **Newport-Inglewood** fault zone. The only M6 or greater earthquake plotted on Plate 4 is the 1933 Long Beach earthquake (Barrows, 1974) . In addition, several major shocks have occurred in the onshore and offshore southern California region. Major earthquakes (estimated or measured M7.0 and greater) in this region are described by **Hileman** (1979) as (1) an 1812 shock, probably located on the **Elsinore** or Newport-Inglewood fault zone, that severely damaged the Mission San Juan Capistrano, (2) an 1857 earthquake, probably located on the San Andreas fault, that affected the northern part of the study area, and (3) a 1940 earthquake of M7.1 that occurred in the Imperial Valley area (**Coffman** and von Hake, 1973).

San Diego and the adjacent region were affected by a "violent" earthquake centered in the San Diego area in 1862. In 1968 the region was shaken by the Borrego Mountain earthquake that had a magnitude of 6.5 and locally caused damage and generated tsunamis in the vicinity of San Diego (**Legg** and Agnew,

1979) . Additionally, activity in northern Baja California on the **Vallecitos-San Miguel** fault system in 1949 (**M5.7**) and 1956 (**M6.8**, and three aftershocks of **M>5** during the past 30 years) has been felt in the San Diego area (Kennedy, 1975) . Damaging earthquakes of unknown intensity also affected the San Diego area in 1852, 1856, 1892, and 1894 (Agnew and others, 1979). Seismicity during 1932-1979 in the offshore San Diego area appears relatively low, with the principal coastal and offshore activity associated with the Coronado Bank fault zone and an unnamed fault located 5 km northeast and parallel to it.

The San Pedro shelf was affected by ten or more earthquakes of $M < 4$ to $M > 6$ in 1933, and a similar number in 1934 (**Hileman** and others, 1973; Greene and others, **1975**). Some of these epicenters are aligned near the offshore Pales Verdes Hills fault and some with the **Newport-Inglewood** zone. A strong earthquake, the Long Beach earthquake of 1933 (**M6.3-6.6**), centered along the **Newport-Inglewood** zone offshore from **Newport**, caused extensive damage in the Long Beach area and was felt as far south as San Diego. Between 1935 and 1941, one shock of $M < 4$ or greater, as well as several lesser shocks, occurred annually in the San Pedro shelf area. Activity from 1942-1951 involved several shocks per year, all of $M < 4$, and the area was relatively quiet seismically from 1951 to 1962 (Greene and **others, 1975**). In 1963, eight earthquakes of $M < 4$ and one **$M < 5$** were reported from the area of the San Pedro **escarpment**; a second cluster of events, some having magnitudes of 4 to 5, occurred here in **1967**. Otherwise, the San Pedro shelf area has remained fairly quiet in recent times.

In summary, the distribution of the epicenters on Plate 4 indicates that the greatest seismic activity has taken place in the northern part of the Catalina block of Greene and others (1979). These events, along with geophysical evidence showing local displacement of the seafloor and Quaternary

sediment, indicate that the Newport-I **nglewood**, Pales Verdes Hills and ancillary faults are active in this area. Also, the relative concentration of epicenters along faults that displace the sea floor in the San Diego Trough and within the southern half of the Pales Verdes Hills-Coronado Banks fault zone reflect active faulting **in** these areas as well. The central part of the Pales Verdes Hills-Coronado Banks fault zone appear relatively "quiet" seismically, suggesting that these faults may **be** locked along part of their extent. Although no fault-generated earthquake is known to have created hazardous conditions in the offshore **Gulf** of Santa Catalina region, any assessment of geological hazards to development should take into account the continuing seismic activity related to known faults, as well as the possibility of damage resulting from a large earthquake in an adjacent area. The effects, other than ground motion, of earthquakes in this region may include seafloor mass movement, sediment flowage, liquefaction, differential subsidence and tsunamis.

Tsunamis

Damage from tsunamis has not been extensive in the southern California coastal region, although shallow flooding of lowland areas and minor damage to small boat moorings, wharfs and similar coastal facilities has occurred. The greatest single tidal excursion of sea level (**1 to 1.5 m**) related to tsunami activity took place on May 22, 1960, and resulted from tsunamis associated with a **M8.5** earthquake in Chile (Van **Dorn**, 1979). At least 19 **tsunamis** have been recorded instrumentally during the 92 year period from 1854 to 1872 and from 1906 to 1979 in the San Diego area (Agnew, 1979). The five largest tsunamis recorded during this period are listed below chronologically with their point of origin (van Dorn, 1979):

- 1) April 1, 1946 - Aleutians
- 2) November 2, 1952 - **Kamchatka**
- 3) July 1, 1956 - Aleutians
- 4) May 22, 1960 - Chile (most severe)
- 5) March 28, 1964 - Alaska

Seven other tsunamis have been observed in the San Diego area since 1854, but none of these caused severe damage (Agnew, 1979). However, several major faults in the offshore Gulf of Santa Catalina region show substantial apparent vertical offset, and the possibility of tsunamis resulting from seismic activity along these faults should be considered in hazards mitigation studies.

Seafloor Instability

Seafloor instability here refers to conditions that could lead to seafloor failure from mass movement and liquefaction. Unstable and potentially unstable seafloor conditions identified **in** the Gulf of Santa Catalina region are associated with subaqueous slides, sediment creep and, to a limited extent, with possible accumulations of shallow gas. Additional information concerning instability in the coastal area adjacent to the Gulf of Santa Catalina and the engineering properties of geologic units exposed in this region is contained in reports by Blanc and Cleveland (1968), Wentworth and others (1970), Morton and others (1973, 1974), Morton (1974), Edgington (1974), Miller and Tan (1976), Tan and Edgington (1976), and Kennedy and others (1977).

Subaqueous sediment slides are mass movements of rigid or **semi-**consolidated masses along discrete shear surfaces, which may be concave upward or planar, with relatively little internal deformation (**Dott**, 1963). Slides

are commonly identified on seismic reflection records by the presence (in **longitudinal** sections) of some or all of the following characteristics: 1) a headscarp where the slip surface extend upward to the floor, 2) **compressional** ridges resulting from small-scale thrusting and folding at the toe of the slide, 3) transverse (tensional) cracks in the body of the slide, 4) evidence of rotation or limited internal deformation of reflectors, and 5) the presence of a slip surface represented by a discrete failure plane or by an intensely deformed zone beneath the slide mass. The term slump is commonly applied to a slide that shows evidence of rotational movement along a curved slip surface. Subaqueous slides may occur on slopes of less than 1 degree, and may range upward in size from tens of square meters to square kilometers in area and more than 100 m in thickness (Moore, 1961; Heezen and Drake, 1964; Lewis, 1971; Hampton and **Bouma**, 1977). Subaqueous sediment flows involve the downslope movement under gravity of water-saturated, unconsolidated sediment; the moving mass may behave plastically or as a very viscous fluid, and movement may be slow or rapid (**Dott**, 1963). The velocity and displacement of flow characteristically decrease gradually with depth below the surface, so that the deposit lacks a distinct slip surface. Subaqueous flow deposits are suggested on seismic reflection records by the presence of 1) anomalously thick, apparently detached sediment masses that 2) lack an identifiable slip plane and 3) show acoustic transparency or chaotic internal structure. Sediment creep in the marine environment is a form of flow; it is a poorly understood and poorly documented phenomenon. As used here, it refers to the slow, more-or-less continuous, downslope movement of the upper layers of unconsolidated sediment and is characterized by **hummocky** sea-floor topography, deformed but identifiable acoustic bedding in the upper sediment layers, a downward decrease in the degree of deformation, and the apparent absence of a

slip surface. Creep may extend to depths of 15-20 **m**, and may affect large areas.

Numerous areas of sediment gravity sliding are mapped in the Gulf of Santa Catalina region, the majority in the northern part between San **Mateo** Point and the San Pedro shelf (pi. 5). These areas, in general, are characterized on high-resolution seismic reflection records by a **hummocky** sea-floor surface and, in the subsurface, by steeply dipping, more-or-less distinct reflections extending upward to or near the sea floor. We believe that these reflections represent geologically young failure planes and that the areas comprise a continuous series of rotated and translated sediment masses. Zones of failure typically occur on slopes of 4 degrees or less, at water depths ranging from 250 **m** to 900 m, and extend to a depth of as much as 50 m below the sea floor. Where their dimensions could be determined from multiple line crossings, they were found to range in area from about one square kilometer to about 12 **km²**. One zone 15 km west-southwest of Point La Jolla may be 18 **km²** or more in area, based on a single line crossing and bathymetric characteristics (pi. 5). Extensive sampling was done for a **geotechnical** and **sedimentologic evaluation** of two areas of failure off San Mateo Point; the results of this study are summarized by Edwards and others (1980).

Two areas characterized on high-resolution seismic reflection records by convex-upward, **hummocky-appearing** bulges of the sea floor and disruption or **loss** of shallow **subbottom** reflectors are interpreted as deposits of sediment gravity flows and slides. These areas are located at or near the base of the slope between Newport Beach and Dana Point, at water depths ranging from about 400 m to 700 m. The larger of the areas was crossed by four lines, and was determined to cover nearly 60 **km²** and to extend to a depth of 40 m or more

below the sea floor. These deposits probably represent repeated episodes of relatively recent, small-scale mass movement.

Rotational **slumps** were noted in six areas (pi. 5). One slump area is located near the base of the San Pedro Escarpment 15-20 km south of Point **Fermin** at water depths of 700 m to 850 m. This area was crossed by three lines, and is estimated to cover 8 to 9 km². The remaining areas are located on the east side of the southern Gulf of Santa Catalina, from just north of Oceanside to the U.S.-Mexico border. Water depths range from 100 m to 700 m. **Two** areas were crossed by **two** or more lines, so that their dimensions could be determined. One, located near the head of Coronado Canyon, covers an area of 6-8 km². The most extensive slump deposits in the region are found in the upper part of La Jolla Canyon. Four **scarps**, extending for about 13 km, are mapped along the south side of the canyon, and three more, extending for about 8 km, are mapped on the north side. The breadth across the canyon of the area affected is about 4 **km**, and water depths over the slump zones range from 100 m to 600 m. Failure planes extend to or near the sea floor, attesting to the **recency** of movement of some blocks; the depth of failure in some places exceeds 40 m, and may extend to 80 **m** or more.

Sediment creep was noted on the east slope of the Gulf of Santa Catalina on six line crossings, four in the southern part of the region between Oceanside and San Diego and **two** off Newport Beach. The zones of creep range from 3 km to 6 km in length (**downslope**) and extend from water depths of 150 m to **nearly** 700 m. Creep in this region appears to affect sediments to a maximum depth of about 20 m below the sea floor; in the areas off Newport Beach and DelMar, creep zones appear to merge downslope with areas of sediment gravity sliding (pi. 5).

Large buried channels, probably reflecting erosion and **infilling** during Pleistocene sea level fluctuations, were mapped in three localities in the Gulf of Santa Catalina region (pi. 5). The largest channel, located at a water depth of about 50 m on the San Pedro shelf, is nearly 2 km across. The extent of this channel **is** unknown as it was identified on only one **line** crossing. It is located near the head of the modern San Gabriel Canyon system, and is presumed to have been associated with that system during Pleistocene time. A second channel, located about 15 km south-southwest of Newport Beach, is believed to have been associated with the Pleistocene Newport Canyon system. This filled channel, crossed by three lines, is about one kilometer wide and 12 km long and lies at water depths ranging from 250 m to 575 **m**. A third channel was identified low on the east slope of the Gulf of Santa Catalina 25 km west-southwest of Oceanside at a water depth of 750 m. This channel is about 1.5 **km** in breadth; its extent and relationship to **pre-**Holocene drainage systems was not determined.

Prominent levees associated with the Newport Submarine Canyon system were mapped on the lower slope and basin floor northeast of Lasuen Knoll and southeast of the San Pedro shelf (pi. 5). These deposits occur at water depths of 450 m to 750 m **or** more; they are characteristically 1-2 km wide and range from 6 km to 11 km in length.

Four other areas of levee development were noted elsewhere in the Gulf of Santa Catalina. One of these, located at a depth of about 1000 m northeast of **Thirtymile Bank** and at least **8** km long, appears to be associated with drainage from **Carlsbad** Canyon; another, located **northwest** of Coronado Bank at a depth of 760 m - 900 m and at least 2 km long, is probably related to sediment transport through Loma Sea Valley.

These levees are Quaternary **in** age and some may be undergoing construction at present. The stability of levee deposits probably varies greatly; however, they characteristically consist largely **of** fine sand and silt size material and may be subject to liquefaction while unconsolidated. Their foundation characteristics should be suspect, especially in an area as seismically active as the Gulf of Santa Catalina, until shown otherwise by engineering studies.

Hydrocarbon Seepage and Shallow Gas Accumulations

Natural gases of **biogenic** and **thermogenic** origin may be present in marine sediments. **Biogenic** gases, principally methane, are derived from bacterial alteration of organic material in sediments. **Thermogenic** gases, dominated by hydrocarbons heavier than methane, are by-products of petroleum formation. The presence of **thermogenic** gases in sediments can reflect an over-pressured zone that is discharging gas into the overlying strata either directly or via a conduit such as a fault or bedding plane. Inadvertent penetration of an over-pressured zone or gas escape conduit **accompanied** by sudden venting of **gas** at the surface can pose a hazard to drilling operations. Additionally, gas **of** either type dissolved in the interstitial pore space of sediment lowers the shear strength of the enclosing sediment and increases likelihood of failure; under some circumstances dissolved gas can liquefy spontaneously when subjected to cyclic loading (Hall and Enslinger, 1979).

Gas in sediments is suggested on medium and high resolution seismic reflection records **by** the presence of amplitude anomalies (apparent as enhanced or "bright" reflectors); the sharp termination or displacement of reflectors, commonly associated with acoustically turbid zones; the absence of surface multiples indicating absorption of the seismic signal (Nelson and

others, 1978); and the presence of "pull-downs" from the decreased velocity of sound in gaseous sediments. Water column anomalies on high resolution seismic records in some cases suggest bubbles in the water **column**, although other phenomena such as kelp and fish produce similar appearing features. Side-scan monographs and underwater video or photographic coverage may show seep mounds or craters on the sea floor, and bubbles. Several lines of geophysical evidence are desirable, and in all cases sampling and **geochemical** analyses are needed to verify the presence of gas and identify its origin.

Wilkinson's (1971) study of California offshore oil and gas seeps shows seepage to have been reported from the San Pedro shelf area near Point **Fermin**, from the northeast slope of San Pedro basin and from near shore in the vicinity of Huntington Beach. Greene and others (1975, p. 65 and pl. 13) report additional seeps off the Pales Verdes Hills between Point Vicente and Point Fermin, where they may be associated with the **Cabrillo** fault zone. Water column anomalies, possibly seeps, are reported by Richmond and others (1981) to be present on the San Pedro shelf in the vicinity of the **Cabrillo** and Pales Verdes Hills fault zones. **Additionally**, acoustic anomalies thought to represent shallow gas occur at **subbottom** depths of 15 to 150 milliseconds at scattered locations on the San Pedro shelf and adjacent slope, commonly associated with the Pales Verdes Hills fault zone.

Elsewhere, acoustic anomalies thought to reflect the presence of gas are reported in isolated localities from the **slope** southwest of Dam Point and Oceanside, at water depths in excess of 500 m and at depths below the seafloor of 50 to more than 350 milliseconds, and **in** sedimentary rocks underlying the shelf and slope off San Diego, at **subbottom** depths ranging from 70 to more than 500 milliseconds (Richmond and others, 1981). Water column anomalies reported on Coronado **Bank** and the shelf to the east, near the southern margin

of the study area, may reflect hydrocarbon seepage in those areas (Richmond and others 1981).

Four small areas of acoustic anomaly possibly representing accumulations of gas in sediments were identified during this study at shallow **subbottom** depths on the San Pedro shelf (pi. 5). Three areas were noted in relatively shallow water 15 to 20 **km** south of Long Beach; two of these are in dipping strata of probable late Tertiary and Quaternary age and one appears to be associated with an offshore extension of the Pales Verdes Hills fault zone. The third area south of Long Beach occurs in horizontally bedded strata of Quaternary age at a **subbottom** depth of 30 to 35 milliseconds. A similar appearing acoustic anomaly was noted about 4 **NM** southwest of Newport Beach 10 to 20 milliseconds beneath the sea floor in flat-lying Quaternary sediments.

A single water column anomaly, possibly a seep, was identified on the San Pedro shelf 9 **NM** south of Long Beach (pi. 5); the anomaly lay above folded and faulted strata of probable late Miocene age, and in close proximity to deformation related to the offshore extension of the Pales Verdes Hills fault zone.

Sediment Thickness and Character

The thickness of unconsolidated sediment in the Gulf of Santa Catalina region is shown on Plate 6. The deposits mapped are those that unconformably overlie pre-Quaternary bedrock on the shelf and upper slope, and are presumed to be **Quaternary** in age. Quaternary and pre-Quaternary deposits could not be reliably separated in the basins and locally on the lower slopes of the region; consequently thicknesses shown in those areas are those of acoustically transparent sediments. (The **acoustic** transparency of these deposits results from the overlap between the velocity of sound in water and

in sediment that is very poorly consolidated and water saturated). **These** sediments are presumed **to** be of late Quaternary, probably Holocene age. The thickness of the Quaternary section on the lower slopes and in the basins of this region is consequently greater in many places than is indicated by Plate 6.

The distribution of Quaternary sediment on the San Pedro shelf is complex, partly the result of ponding of sediment in the lee of bedrock irregularities produced by faulting. Generally, **Quaternary** sediment is thin or absent over much of the San Pedro shelf west of the Pales Verdes Hills fault zone, but locally exceeds 20 m in thickness farther east. A bedrock ridge extends from Point Fermin southeastward along the west side of San Gabriel Canyon; this ridge, formed by displacement along the Pales Verdes **Hills** fault, appears to have acted as a barrier to sediment dispersal during Quaternary time. The thickest deposits on this shelf segment occur near the shelf break between the San Gabriel and Newport Canyon systems (pi. 6). Quaternary sediment cover on the shelf segment between Newport Beach and Point La Jolla is thin, generally less than 10 m. Locally, as off Dana Point and between San Mateo Point and Oceanside, these deposits reach 15 m to 20 m in thickness (pi. 6), probably reflecting the damming of littoral drift by projecting headlands and the proximity of sediment sources to the shelf (e.g. , San **Mateo** Creek, San Onofre Creek, Las **Pulgas** Creek, and the Santa Margarita River). Quaternary sediment is thin, commonly less than 5 m thick, **over** most of the San Diego shelf. A prominent bedrock high extends from seaward of Point La Jolla along the coast to and southward from Point **Loma**; a second bedrock ridge extends along the outer shelf between Point Loma and Coronado Canyon (pi. 6).

Quaternary slope deposits are thin, characteristically 5 m to 10 m or

less in thickness. Deposits are thickest where slopes are moderate off river mouths and in the vicinity of canyons (e.g., off Newport Beach and Oceanside, pl. 6). Many steeper slopes appear devoid of Quaternary sediment other than a thin **hemipelagic drape**. These deposits thicken **basinward**, and ultimately merge conformably with late Tertiary sediments from which they **could** not be separated on high-resolution seismic profiles.

Sediment types and sources in this **region** are mapped by **Welday** and Williams (1975) and are discussed by Emery (1952, 1960), Stevenson, **Uchupi** and **Gorsline** (1959), **Wimberly** (1964), and **Gorsline** and Grant (1972). Quaternary sediment on the San Pedro shelf consists principally of fine sand and silt, with some coarse relict beach or terrace deposits along the western edge, **detrital** sand seaward of the Santa Ana and San Gabriel Rivers, and fine **detrital** silt and clay along the inner shelf **between** about San Pedro and the mouth of the San Gabriel River (Moore, 1954; **Uchupi** and **Gaal**, 1963; Bandy and others, 1964; **Gorsline** and Grant, 1972). The principal sources of modern sediment on the San Pedro shelf are the Los Angeles, San Gabriel and Santa Ana Rivers (**Gorsline** and Grant, 1972).

The shelf segment between Newport Beach and La Jolla is **characterized by** fine sand to silt-size material, with admixtures of fine to medium sand adjacent to the mouths of rivers supplying sediment to the shelf, and relict sand locally along the shelf edge. Well-sorted, fine- to medium-grain sand typically covers the San Diego shelf at water depths shallower than 20 m; these sands grade seaward to silt-size material at greater water depths (Henry, 1976). Relict gravels are present locally along the shelf edge and on topographic highs (Henry, 1976). The principal sources of sediment on the present day San Diego shelf are the San Diego and **Tijuana** Rivers (Henry, 1976) .

Summary of Hazards

Several geologic features and conditions in the Gulf of Santa Catalina region **merit** special attention, as they are potentially hazardous to offshore development. Foremost among these are active faulting, **seismicity** and sea-floor instability. Prominent, geologically young faults that displace the sea floor or cut Quaternary sediments occur (1) on the inner shelf from north of Oceanside to Point La Jolla along the Newport-Inglewood-Rose Canyon fault zone, (2) on the San Pedro shelf and in the Gulf of Santa Catalina from Lasuen Knoll to Coronado Bank along the Pales Verdes Hills-Coronado Bank fault zone, (3) in the Gulf of Santa Catalina and on the San Diego shelf along **two** unnamed fault zones 30-50 km long lying between the **Newport-Inglewood-Rose** Canyon and Pales Verdes Hills-Coronado **Bank** fault zones, (4) in the northern and central San Diego Trough along San Diego Trough fault zone, and (5) along the northeast flank of **Thirtymile Bank (pls. 4, 5)**. These groups of faults probably reflect a broad zone of active shear [pi. 4]. Additionally, the San Pedro shelf off Newport Beach was the site of a strong **(M6.3-6.6)** earthquake on the **Newport-Inglewood** fault zone that caused considerable damage in the Long Beach area in 1933.

The region is seismically active, especially the northern part in the vicinity of the Los Angeles Basin and adjacent offshore areas. Epicenter plots attest to recent movement on faults in the **Newport-Inglewood**, Pales Verdes Hills and Coronado Bank fault zones, on an unnamed fault lying about 5 **km** northeast of, and parallel to the Coronado Bank fault, and possibly on the Rose Canyon fault zone (pi. 4). In addition, this offshore region has been shaken by numerous moderate and major earthquakes in adjacent onshore areas of southern California and northern Baja California during historic time.

Associated with the hazards of faulting and **seismicity** are those resulting from ground shaking and seafloor mass **movement**, sediment **flowage**, and liquefaction. Evidence of geologically young sea-floor mass movement is common on high-resolution seismic reflection records from this region (pi. 5), and slopes sufficient to promote failures in unconsolidated sediments are present flanking the mainland shelf, Catalina Island, **Thirtymile** Bank, and the several bedrock knolls in the Gulf of Santa Catalina. The presence of gas in sediments reduces their bearing strength, contributing to the possibility of failure. Evidence of shallow gas and hydrocarbon seepage has been noted in Quarternary sediments on the San Pedro shelf in this study and in studies by Wilkinson (1971), Greene and others (1975) and Richmond and others (1981), and elsewhere on the mainland shelf and Coronado Bank by Richmond and others (1981).

Large sediment gravity **slides** up to 12 km² or more in area and extending to **subbottom** depths of 50 m or more are mapped on slopes flanking the mainland shelf between Newport Beach and SanMateo Point, and off Point La **Jolla** (pi. 5)* **Geotechnical** and **sedimentological** studies of two slide areas off San Mateo Point **were** carried out in conjunction with this study; the results are reported by Edwards and others (1980). Rotational slumps are mapped at isolated localities throughout the region, but are most numerous along the southeast margin of the Gulf of Santa **Catalina**, from just north of Oceanside to the **U.S.-Mexico** border (pi. 5). The most extensive slumping occurs in the upper part of La Jolla Canyon, where 7 scarps are mapped for 13 km or more along the canyon margins. Failure planes associated with these slumps locally cut the sea bottom to a depth of 40 m or more. An extensive area interpreted as the deposits of sediment gravity flows and slides that are no longer active is mapped on the mainland slope between Newport Beach and Dana Point, and

evidence of sediment creep was noted in seismic reflection records from isolated localities along the mainland slope throughout the region (pl. 5).

CENTRAL SANTA ROSA-CORTES RIDGE

Introduction

The central Santa **Rosa-Cortes** Ridge includes the bank tops, slopes and basin margins of the Ridge, the San **Nicolas** Island platform, and Dan and Nidever **Banks**. The study area extends from approximately 33°44'N on the north to 32°45'N on the south, and from **119°00'W** on the east to **120°00'W** on the west (fig. 2).

The morphology of the study area is shown in Figure 2. The San **Nicolas** Island platform is a broad, flat, 50 to 200 **m-deep** shelf extending northwest from the island. San **Nicolas** Island extends nearly 300 **m.** above sea level in the southeast part of the platform. Elsewhere, the central Santa **Rosa-Cortes** Ridge lies at greater depths and is more irregular, especially in the vicinity of Dan Bank. The ridge is flanked by moderate to steep slopes that range in declivity from about 2° to 20°. Most slopes are in the range from 3° to 13°, and the average slope is about 8°. Slopes flanking the central Santa **Rosa-Cortes** Ridge are incised by numerous canyons, gullies, and sea valleys.

A geophysical **reconnaissance** of this area was made by the USGS aboard the R/V KELEZ in **1973**. Additional seismic reflection lines and a series of gravity cores and grab samples were obtained from the San **Nicolas** Island platform and adjacent slopes aboard the USGS vessel R/V LEE in 1976; however, the majority of data used in this report were obtained in 1978 aboard the R/V SEA SOUNDER. During the latter cruise, data from 160 **kJ** single channel sparker, **Uniboom**, and **3.5** kHz profiler were obtained simultaneously on a series of profile lines covering the entire study area (**pl.7**).

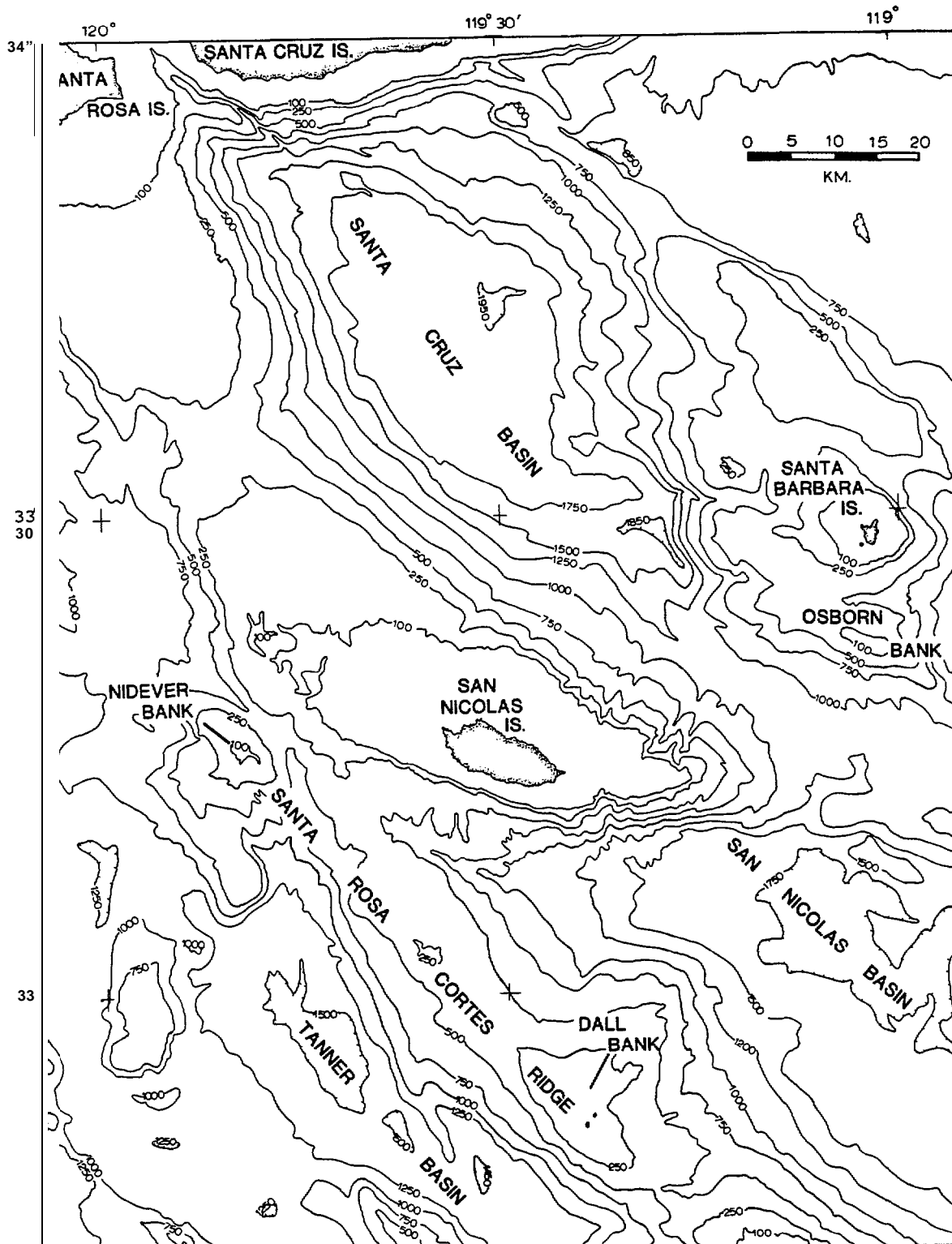


Figure 2. Location map, central Santa Rosa - Cortes Ridge area.

Geologic Structure

Vedder and others (1974) have described the Santa Rosa-Cortes Ridge as "the most persistent geomorphic feature east of the Patton Escarpment." The ridge extends from Santa Rosa Island on the north to the southeast end of **Cortes** Bank, a distance of over 200 km. Flat topped and asymmetric in **cross-section**, the ridge includes San **Nicolas** Island and its surrounding platform shelf, which form an east southeast-trending salient. The structure, rocks, and sediment of the Santa **Rosa-Cortes** Ridge have been studied by Emery (1960), Moore (1969), **Uchupi** (1961), Vedder and Others (1974), Vedder (1976), **Arnal** (1976), Field and Richmond (1980) and Greene and others (1975). Much of the most recent and comprehensive information on **stratigraphy** and structure appears in Vedder and others (1974) and the following discussion is capsulized from their work.

The Santa **Rosa-Cortes** Ridge is a broad **anticline** composed of Tertiary sedimentary rock, with a complex pattern of faults and minor folds superimposed on the main northwest trend. The platform shelf of San **Nicolas** Island consists of out-cropping Eocene siltstone and sandstone that are thinly veneered by Quaternary sediment. Eocene rocks also crop out locally in the vicinity of Dan and **Nidever** Banks (fig. 2; pl. 8). Northwest and southeast of San **Nicolas** Island, the top of the ridge **is** composed of lower, middle, and upper Miocene sedimentary rocks, and volcanic rock of Miocene age is present in isolated exposures along the ridge. Pliocene rocks are uncommon along the ridge top, but crop out on the upper slopes of both flanks of the ridge. The lower slopes of the Santa **Rosa-Cortes** Ridge and the adjacent basins contain appreciable thicknesses (>100 m) of Quaternary **mudstone** (pi. 8).

The geology of San **Nicolas** Island has been described by Vedder and Norris (1963) and Cole (1970, 1977). The island is underlain principally by

interbedded marine sandstone and siltstone of Eocene age that are capped by Quaternary dune and terrace deposits. The exposed Eocene rocks comprise a marine section more than 1000 thick that crops out along the flanks of a broad, complexly faulted, southeast-plunging **anticline**. **Two** major sets of intersecting faults trend approximately **N30°W** and **N80°E** and offset the axis of the major **anticline**. These faults appear to be contemporaneous and probably are **pre-middle** Miocene in age, although **lesser** fault movements occurred through late Pleistocene time. Diving observations by Vedder and Norris (1963) and Menard and others (1954) indicate the structure of the shelf northwest of San **Nicolas** Island to be similar to that on the island itself. Faults mapped offshore in this study also have trends that are similar to those observed on the island. Vedder and Norris (1963) note that, in addition to the evidence of recent tectonic activity from fault separations in Pleistocene deposits on San **Nicolas** Island, significant uplift of marine terraces has occurred around the island. Elevations of these terraces do not correspond to Pleistocene eustatic levels, indicating that appreciable uplift has occurred in the past **two** million years.

The structure of the central Santa Rosa-Cortes Ridge is shown on Plate 9. Fold patterns generally conform to the major trends identified by Weaver and **Doerner** (1969), Moore (1969) and Vedder and others (1974). The northwest-trending **anticline** forming the axis of San **Nicolas** Island swings northwestward offshore, merging with the northwest-trending structural grain of the central Santa **Rosa-Cortes** Ridge. Minor folds south and north of the island and on the adjacent slopes and basins generally conform to these trends (pi. 9). Orientations shown for short fault traces on Plate 9 are based on single **trackline** crossings and on inferences from topographic trends, hence are less reliable than orientations shown for longer fault traces that have

been correlated between adjacent **tracklines**. With few exceptions, faults that can be correlated between **tracklines** are interpreted as conforming to the general west to northwest trend of the principal structural fabric of the ridge.

Seismic hazards

Faults. Many of the morphologic features on the central Santa **Rosa-Cortes** Ridge reflect faulting. Most notably, the south side of the San **Nicolas** Island platform is bordered by **scarps** formed by west-trending faults that swing gradually northwestward as they merge with the ridge proper.

Approximately **24** faults of those shown on Plate 9 displace the seafloor. Most faults displacing the sea floor are shown as pre-Quaternary in age, as much of the sea floor on the ridge and bank tops is exposed Tertiary bedrock. Whether this merely reflects the thinness **or** absence of Quaternary sediment or is a true indication of the age of faulting is difficult to establish. The angularity in seismic profiles of some sea-floor **scarps** implies that some displacement may be Quaternary in age, and on the lower slopes and basin floors where Pleistocene and Holocene fine-grained sediments are prevalent **numerous** faults of Quaternary age are mapped.

Most faults displacing Holocene and Pleistocene sediment on the sea floor show less than 10 m of vertical separation. Older faults that displace the sea floor (e.g., the fault bordering the south side of the San **Nicolas Island** platform) may have up to several hundred meters of vertical offset, although most show vertical offsets of less than 50 m. The style of faulting is not readily apparent from seismic reflection data. Field and Richmond (1980) suggest that strike-slip faulting has occurred on the northern Santa **Rosa-Cortes** Ridge. Right-lateral strike slip probably is the principal type of

fault movement in the southern California borderland and the adjacent onshore region, and it is likely that this style of faulting is prevalent in the central Santa Rosa-Cortes Ridge and San **Nicolas** Island area as well. This is significant in that faults displaying minor apparent vertical separations also may have major components of lateral separation.

Seismicity. Earthquake activity in the outer borderland has been monitored by the California Institute of Technology since 1932 (**Hileman and others, 1973**). In 1960, the USGS established a seismograph **network** in the vicinity of the Santa Barbara channel that allowed the recording of events along the Santa **Rosa-Cortes** Ridge. Data from these two sources form the basis for interpretation of **seismicity in** this region.

Numerous small to intermediate earthquakes have occurred within 100 km of the central Santa **Rosa-Cortes** Ridge during the nearly 48 year interval **between** January 1, 1932 and September 30, 1979 (p. 10). Most of the 151 seismic events recorded for this area have had an estimated magnitude of less than 4 on the Richter Scale. **Ten** earthquakes have had a magnitude in excess of 4 and three of these were greater than 5.

TABLE 1. Earthquakes in the vicinity of the central Santa **Rosa-Cortes** Ridge (1932-1979)

<u>Magnitude</u>	<u>No. of Events</u>	<u>Avg. No. per Decade</u>
< 2.9	59	10.2
3.0-3.9	82	17.1
4.0-4.9	7	1.5
5.0-5.9	3	0.6

Earthquakes of greater than 5 magnitude occurred at distances of 2 and 25 km from San **Nicolas** Island in 1947 and 1969, respectively.

Epicenter locations shown in plate 10 do not demonstrate a pattern that can be related to known faults or **landforms**. The majority are shown to have occurred east of San **Nicolas** Island in the vicinity of the west flank of the **Osborn** Bank and the Santa Barbara-San Clemente Ridge. The apparent lack of epicenters on the central Santa Rosa-Cortes Ridge **may** result in part from the relatively great distances to recording stations and the resultant imprecision in epicenter location. Lee and Vedder (1973) compared epicenter locations in the Santa Barbara Channel region, as determined by the California Institute of Technology and **U.S.G.S.** data sets. Their **analysis** shows local discrepancies of as much as 39 km between the two sets of solutions. This difficulty in accurately establishing the locations of earthquakes increases in the more remote areas of the California continental borderland. The primary value of the data presented in Plate 10 lies in their indication of the frequency and magnitudes of earthquakes that have occurred in this region.

Seafloor Instability

Slopes in the southern California borderland are avenues of mass transport of sediments to the adjacent basine (Field and Edwards, 1980). Although sediment sources in the central Santa **Rosa-Cortes** Ridge area are limited, particularly since the most recent eustatic rise in sea level, a combination of factors including the presence of unconsolidated sediments, relatively steep slopes, and moderate seismic activity have acted to produce numerous small slides and flows (pi. 11). Slumps (rotated slides) are identified on seismic reflection records as discrete sediment packages with **hummocky** or mounded upper surfaces, and chaotic or rotated internal reflectors. Most slumps in the study area are 0.5 to 5 km in width. They occur on slopes of varying declivity, but are more commonly recognized on the more gentle slopes. Using a deeply-towed acoustic source, Field and Clarke

(1979) identified six small failure zones that had not been recognized by use of surface-operated equipment. All the zones lie within a **small** (150 km²) **intercanyon** segment of the slope east of San **Nicolas** Island; each is different in size, geometry, age, and probable mechanism of failure. **Because** of the relatively small size of failures mapped on Plate 11, the density of mapped failures reflects to a large degree the trackline spacing and quality of **high-resolution** seismic reflection **data**. Failure zones marked with an "F" on Plate 11 are interpreted as flow deposits. Flow deposits commonly are thin, acoustically transparent, and are bounded by a rounded nose or curved surface on the **downslope** side. Their identification is difficult because they lack other diagnostic features. Consequently, flow deposits may be more abundant than shown on Plate 11, particularly in the adjacent basins, which are presumed to be the sites of deposition for most flows generated on the adjacent slopes (**Gorsline**, 1980; Field and Edwards, 1980).

Studies of **planktonic** Foraminifera populations from cores on the slopes of the Santa **Rosa-Cortes** Ridge show that sediment mixing by small-scale gravity transport is ubiquitous. These analyses by G. Keller (written commun., 1977) show that modern slope sediments contain an appreciable amount (commonly more than 50 percent) of **reworked** Foraminifera, i.e., broken, abraded, and stained Miocene tests that are admixed with a population of Quaternary **Foraminifera**. Miocene strata are exposed on the upper slopes and edges of the ridge, and these strata are presumably the source for the reworked fauna (Field and Edwards, 1980). The frequency of sediment failures on the slope is not known. Those mapped are all Quaternary in age, but whether they are all related to lower stands of sea level is not **clear**. The freshness of many of the failures indicates that they are geologically young, and some may have occurred within historical time. Moreover, undisturbed

Holocene fine-grained sediment is present on many steep slopes in the study area, and there exists a potential for future failures **in** these deposits.

In addition to evidence of mass transport on smooth slopes, a large number of canyons and channels incising the slopes appear to be active conduits for channelized flows. The presence of sharp, well defined channels, levee systems, and coarse sediments in canyon axes all suggest that sediments periodically are transported through these channel systems to the adjacent basins.

Hydrocarbon Seepage and Shallow Gas Accumulations

Only one area was identified as having acoustic anomalies that might reflect shallow gas accumulation. The area was noted on **two** intersecting profile lines and lies on the shelf west of San **Nicolas** Island (pi. 11). The appearance of these anomalies, coupled with the shallow water depth (50 meters), suggests that they may be caused by kelp rather than by gas; however, this could not be resolved with the data available.

No evidence of shallow gas accumulation in sediments was noted in seismic reflection profiles collected for this study in the Dan **Bank** area. However, examination of closely spaced lines in this area by Richmond and others (1981) indicates that **two** small zones of shallow gas and seeps and seep mounds are present in six tracts offered for sale in OCS lease sale 48. Seeps from both bedrock and unconsolidated sediment **were** noted, and some seeps appear to be associated with faults.

Sediment Character and Thickness

Little information has been published about the character and thickness **of** the sediment cover on the Santa Rosa-Cortes Ridge or San **Nicolas** Island

platform. **Uchupi** (1961) reported results of selective grab samples along the ridge and Norris (1951) reported the **lithology** of samples collected from the shallow platform shelf around San **Nicolas** Island.

Analysis of high-resolution records collected for this study indicates that modern sediments are exceedingly thin or absent on the ridge crest. Those areas generally having less than 2 m of unconsolidated sediment cover are shown in Plate 11. The irregularity of the shelf surface in these areas indicates it is composed mostly of outcropping Tertiary bedrock with essentially no sediment cover. Along the shelf edge south of the island lies a long, thin band of sediment that is between 5 and 10 m thick (pi. 11). This band is the only significant accumulation of modern sediment on the ridge top.

Welday and Williams (1975) have compiled available sediment information to produce a map showing the distribution of various sediment types along the entire California continental margin. The results of USGS sampling within this study area agree closely with this map. The map of **Welday** and Williams (1975), modified to reflect sample data obtained by the USGS in 1976 and data reported to the Bureau of Land Management (**BLM**) by Science Applications, Inc., is shown as Plate 12. The shallow areas of the ridge and island platforms are shown to be areas of outcropping bedrock having a thin veneer of predominantly sand-size material. Deeper areas on the axis of the ridge contain bands of fine sand, and the upper slopes are characterized by a mixture of mud with lesser amounts of sand. The lower slopes and basins contain thick sequences of very **fine-grained** sediment, dominantly fine silt and clay. Barnes (1970) reports average grain sizes of 5 to 10 microns for sediments on the lower slope and basin east of San **Nicolas** Island.

Mean grain size and percent each of sand, calcium carbonate, and organic carbon for samples collected by the USGS in 1976 and data reported to the **BLM** by Science Applications, Inc. is presented in Plate 13. Many samples

collected **from** the shelf around San **Nicolas** Island contain **clasts** and rock fragments in addition to the high proportion that are **predominantly** sand. The percent sand figures reflect the coarseness of shelf and ridge sediments; the presence of coarse sediment in canyons and on slopes also reflects the **downslope** movement of shelf sediments (pi. 13). The calcium carbonate values show that a high proportion of **biogenic** material, chiefly **Foraminifera**, is present in modern sediments on the ridge and adjacent slopes.

The thinness and nature of surficial sediments on the Santa Rosa-Cortes Ridge and the San **Nicolas** Island shelf indicate that present deposition is minor. Sediments are reworked by long-period waves and major cross-ridge currents resulting in a thin sandy lag deposit that has a large component of **biogenic** material. Silt eroded from the ridge top presumably is deposited in basins and on the adjacent slopes. Coarser materials are carried in a traction layer across the shelf, predominantly to the eastern edge, where they are transported down canyons and gullies and down slope by processes of mass movement (Field and Edwards, 1980).

Summary of Hazards

The central Santa **Rosa-Cortes** Ridge and San **Nicolas** Island platform are situated in a widely varied tectonic and sedimentary environment. Faults are common throughout the area on the ridge top, on the flanking slopes, and in basins. Activity along major faults has created major geomorphic features, such as scarps. The ages of many faults on the truncated, current-swept ridge top are uncertain, but displacement of the sea floor and Quaternary sediments on lower slopes and basin floors indicates Quaternary fault movement. Additional evidence **of** recent tectonic activity is reflected by historical epicenter data. Although earthquake activity is moderate relative to other parts of the borderland, there have been over 150 recorded seismic events in

the past 48 years, ten **of** them between 4 and 6 in magnitude. These events have the capability of inducing fault movement, ground shaking, and sediment failure by liquefaction and mass movement.

The platform shelf around San **Nicolas** Island and the crest of the Santa Rosa-Cortes Ridge are nearly devoid of sediment except for a thin veneer of sand and gravel, indicating minor sediment input and strong scour by currents. The steep slopes of the ridge are composed of unconsolidated clayey silts that are failing and moving **downslope** as slides and flows. The ages of failures are not well established but the abundance of failures suggest that processes of mass movement are presently active. These slopes are incised by numerous gullies, canyons, and sea valleys that show evidence of recent **channelized** flows.

WESTERN SANTA BARBARA CHANNEL -

POINT CONCEPTION REGION

Introduction

The region studied lies in the extreme northwestern part of the southern California borderland, in the **western** Santa Barbara Channel. It comprises an area of approximately 12,750 **km²** that extends offshore and southwestward from Point Conception and Point **Arguello**, and lies to the north and west of San Miguel Island (fig 3). Geophysical data were collected from the narrow continental shelf and from the northern Channel Islands platform and continental slope, at depths ranging from 50 **m** to over 2500 m.

The offshore Point Conception area is **physiographically** complex. The shelf that fronts the shoreline between Point Conception and Santa Barbara is narrow, generally less than 6 km wide. This shelf widens as it swings

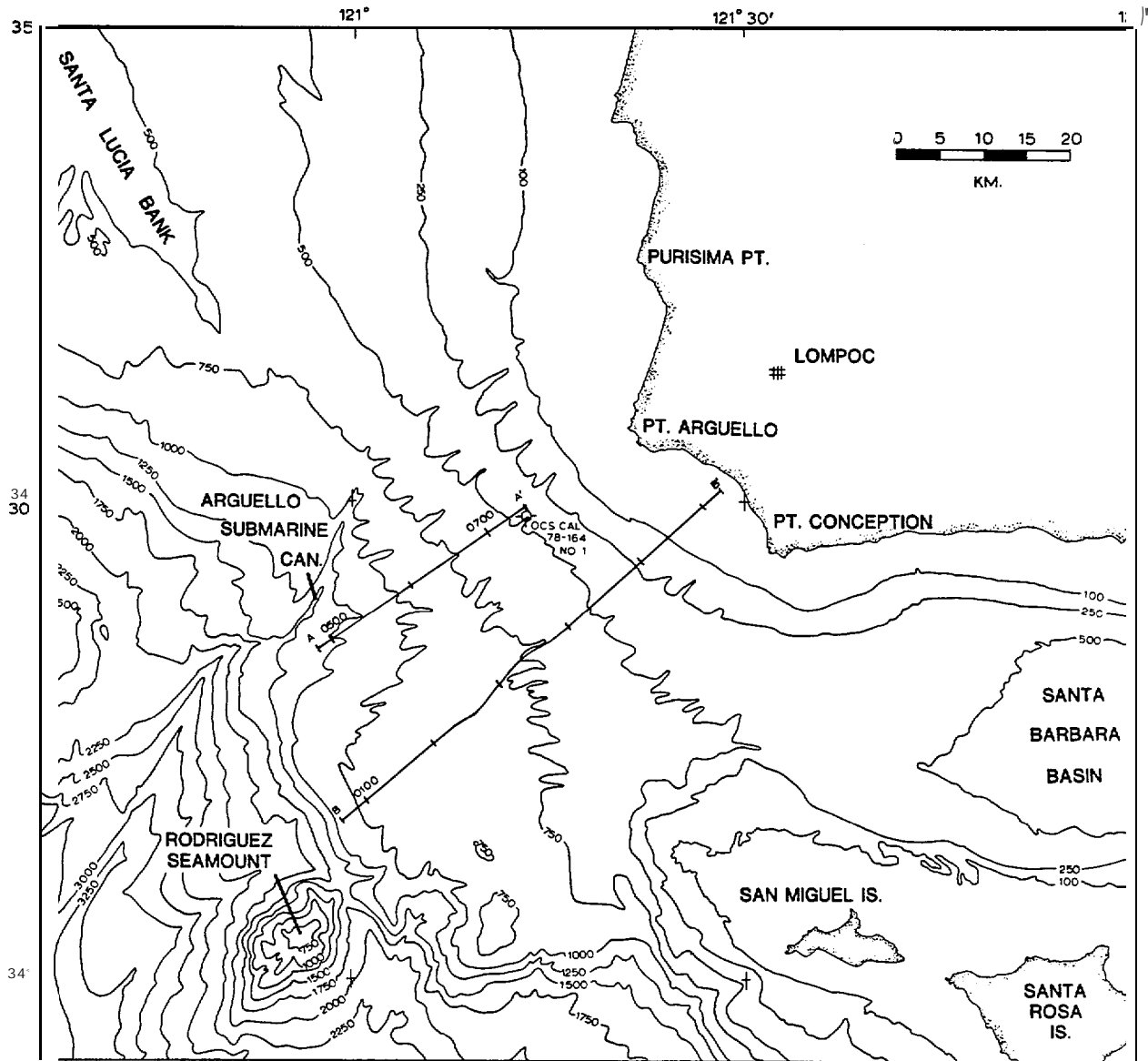


Figure 3. Location map, western Santa Barbara Channel - Point Conception area. Interpreted seismic reflection profiles A-A' and B-B' are shown in figures 4 and 5.

westward and northward around Point Conception, and is nearly 20 km wide offshore from the Santa Maria area. The shelf break is sharp and well defined at the 100 m contour, **where** a 20 to 60 m **scarp** exists. West of Point Conception, past the western sill of the Santa Barbara Basin, the slope is wider and less steep than in the Santa Barbara Channel.

The continental slope seaward of Point **Arguello** and Point Conception is incised by the many heads of **Arguello** submarine canyon. These tributaries notch the seaward edge of the shelf at or near the 100 m **scarp**. The canyon heads form a radiating pattern, with their prevalent orientation swinging from nearly west in the northern part of the region to nearly south in the southern part.

Data used in this study were collected during the May-June, 1978 cruise of the R/V SEA SOUNDER (USGS Cruise **S2-78-SC**); **trackline** locations from this cruise are shown as Plate 14. A preliminary geologic map (pi. 15) was constructed from shallow-penetration, high-resolution (**Uniboom**) continuous seismic reflection profiles. Deep-penetration, **low-resolution** reflection profiles collected simultaneously were used to correlate deep structures with shallow features observed in the high-resolution data. Maps depicting bottom morphology and thickness of Quaternary sediments were also compiled from the geophysical data (**pls.** 16 and 17). Faults mapped from these data are compared with earthquake epicentral data in a map showing faults and seismicity for the region (pi. 18). Other geophysical profiles were used to fill data voids and to more accurately correlate major structures. Intermediate-penetration, **low-resolution** sparker profiles collected by the USGS aboard the R/V POLARIS in 1972 (Wolf, 1975), Bendix (Marine Advisors) data collected in 1970 and reported on by MESA, Inc. (1978) and Dames and Moore (1978), and side-scan sonar profiles collected by **B. P. Luyendyk** and D. S. Simonetti in 1977 and

1978 under Sea Grant **Number** R/E 18 were used to fill in structural detail on the continental shelf east of Point Conception, **Preliminary** interpretations of intermediate-penetration and high-resolution, digitally processed sparker profiles collected by McClelland Engineers in 1979 for the USGS-Conservation Division (USGS Data Set PA 17200) were used to map structure along the northern margin (slope) of the Western Santa Barbara Basin. Structure in the shallow subsurface **was** correlated with that in the deeper subsurface by comparing deep-penetration **CDP** multi-channel profiles with intermediate- and **shallow-penetration** profiles. Side-scan sonar profiles were studied for **surficial** evidence of sea floor instability and faulting on the continental **shelf** east of Point Conception.

Seismic Interpretations

Five major acoustic units have been identified in the seismic reflection profiles used in this study; these units are correlated with acoustic units A through E defined by **McCulloch** and others (1979) from CDP multi-channel seismic-reflection data. Apparent ages of structures identified in the profiles are based on the correlation of these acoustic units with core hole samples obtained from the Point Conception deep stratigraphic test well **OCS-CAL 78-164 No. 1** (Cook, 1979). Offshore acoustic units were also correlated with rocks exposed onshore, where possible, and with sea-floor samples. Line drawings were made for most of the 1978 USGS seismic reflection profiles; two of these drawings are included in this report as Figures 4 and 5. The location of these line drawings is shown in Figure 3.

McCulloch and others (1979) have defined acoustic units in a CDP multi-channel seismic reflection profile across the continental slope of the Point Conception region, and have correlated them with **lithostratigraphic** units

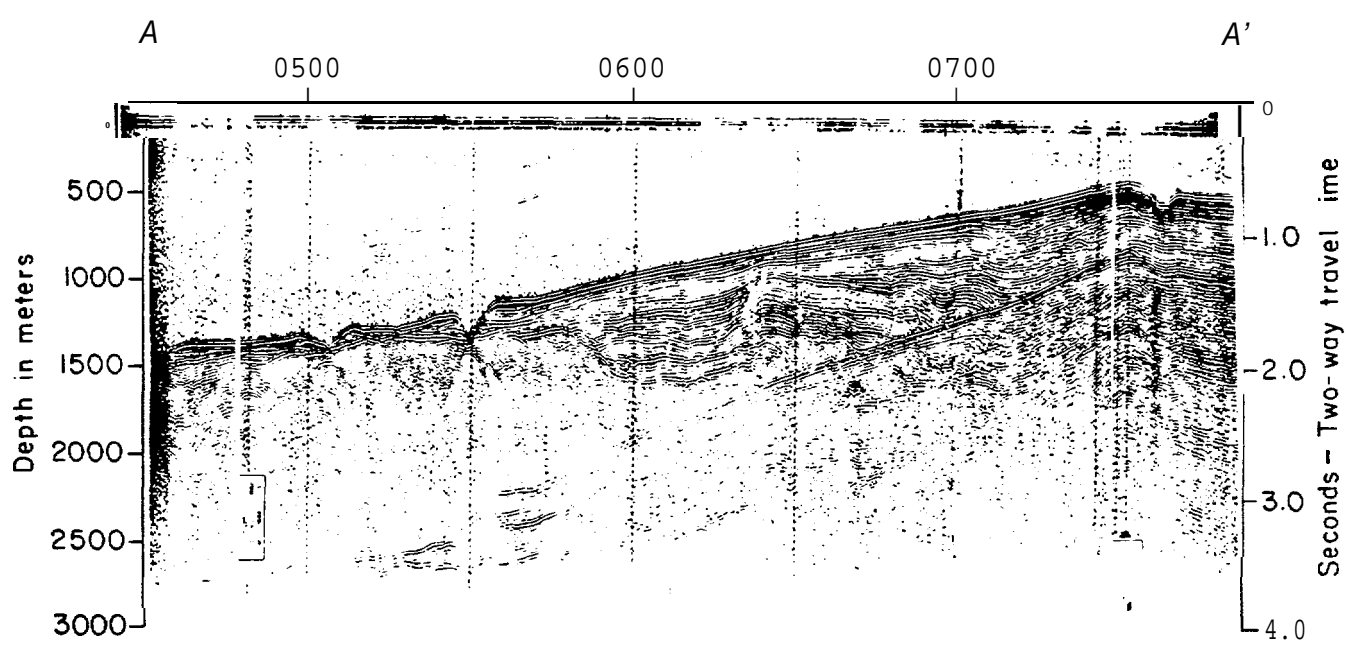
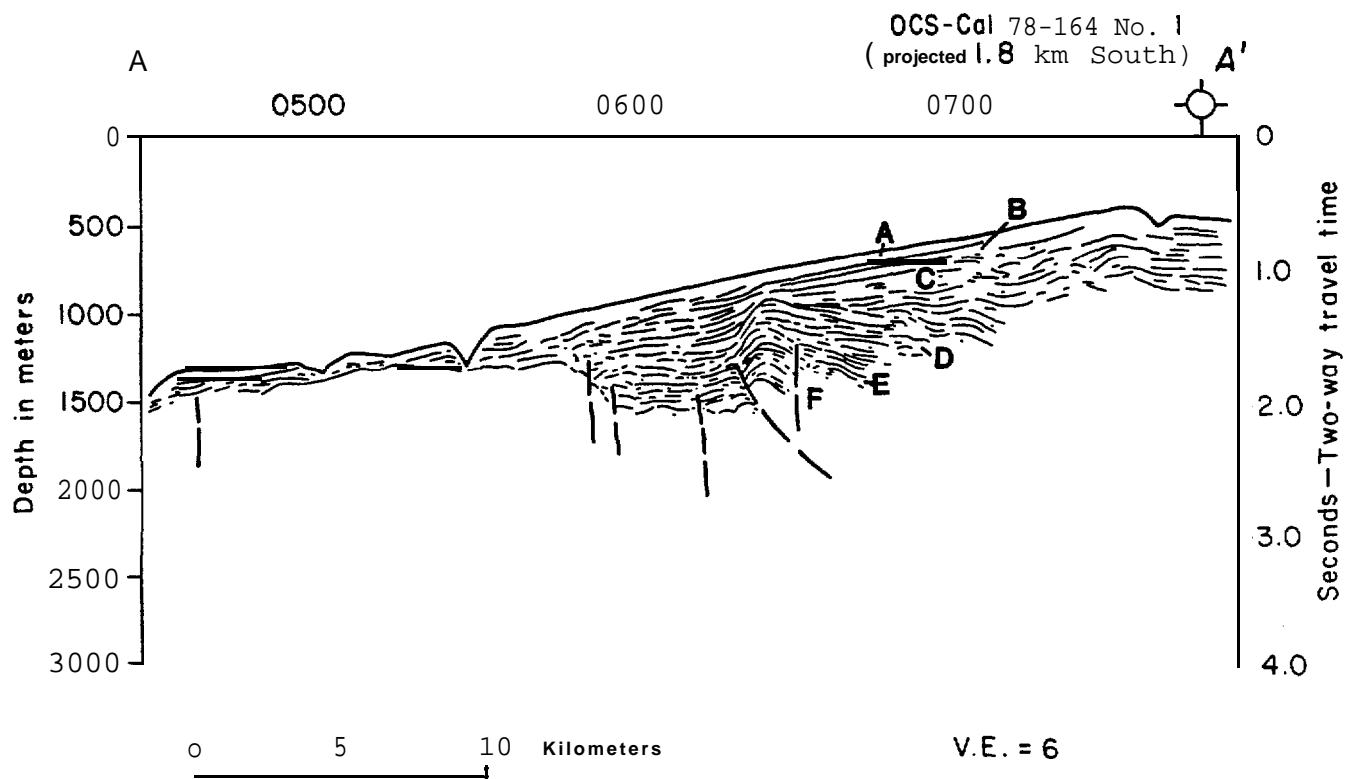


Figure 4, Interpreted seismic reflection profile (line 131, S2-78SC). See Figure 3 for location.

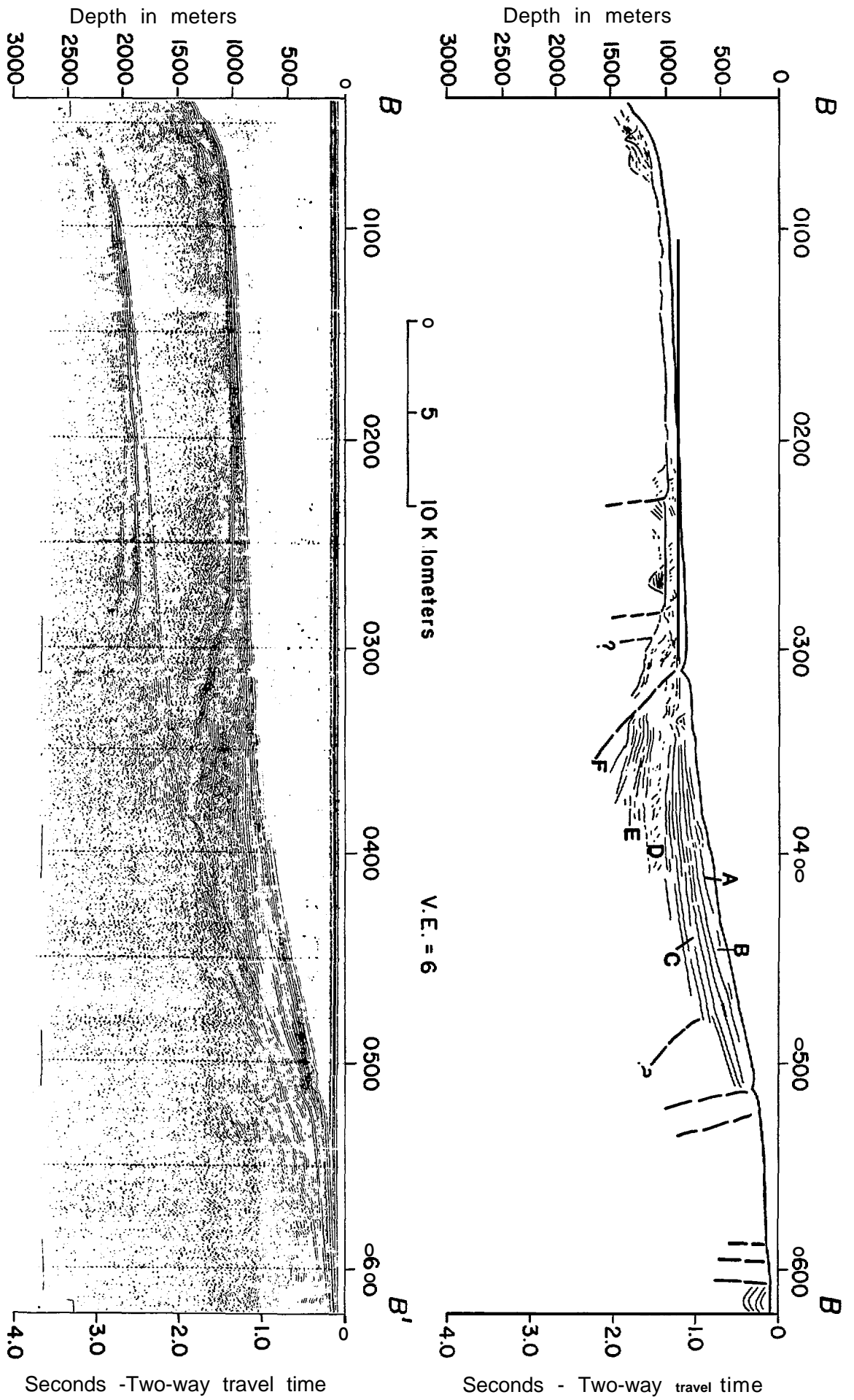


Figure 5. Interpreted seismic reflection profile (line 114, S2-78SC). See Figure 3 for location.

sampled in the Point Conception deep **stratigraphic** test (COST) well **OCS-CAL** 78-164 **No. 1**. This acoustic **zonation** has been applied to the profiles used in this study. Acoustic units A through E, as used in this report, are described below:

Unit A - This unit is about 0.10 sec (2-way travel time) thick and is generally masked by the bubble-pulse in our seismic reflection profiles (figs. 4, 5). The base of this unit is locally defined by a high amplitude reflector that correlated with the base of **McCulloch and others'** (1979) acoustic unit **A** on the basis of **2-** way travel time. The age of this unit is Quaternary and **it** apparently includes sediments of both Pleistocene and Holocene age.

Unit B - This unit comprises a package of relatively strong and continuous reflectors that remain an approximately uniform thickness in seismic reflection profiles. The base of this unit lies at a depth of about 0.24 sec (2-way travel time) beneath the sea floor, and marks a change in acoustic character from continuous well-layered reflectors to discontinuous, weak and somewhat contorted reflectors. **McCulloch** and others (1979) indicate that this boundary marks a change in **lithology** from predominately silty **claystone** of late Pliocene to Quaternary age (unit B) to conglomerate and silty sandstone of late Pliocene age (unit C).

Unit C - This unit comprises an interval of low amplitude, locally folded, discontinuous reflectors that vary in thickness and

unconformably overlies an interval of more continuous, higher amplitude reflectors. This unit is described by **McCulloch** and others (1979) as a silty sandstone of late Pliocene age; it is marked at its base by a high amplitude reflector at a depth of approximately 0.75 sec (2-way travel time) beneath the sea floor. This horizon in the COST well marks a change *in lithology* from sandstone and conglomerate (unit C) to **calcareous** sandstone and shale (unit D). **McCulloch** and others (1979) suggest that this unit may be the offshore equivalent of the **Careaga** Sandstone of the Santa Maria basin.

Unit D - This unit is a package of acoustically continuous, **high-** amplitude reflectors. The base is difficult to define, and is based on seismic travel time; it lies at a depth of nearly 1.2 sec (2-way travel **time**) beneath the sea floor. The unit is represented in the COST well by a **calcareous** siltstone that **McCulloch** and others (1979) suggest may be the offshore equivalent of the Foxen Mudstone of middle (?) to late Pliocene age.

Unit E - This unit is comparable to unit D in acoustic character. It contains high-amplitude, continuous reflectors that are slightly distorted near the base. The base of the unit is defined by a **very** high-amplitude reflector that marks the surface of the acoustic basement in our profiles. This surface lies at a depth of nearly 1.7 sec (2-way travel time) beneath the sea floor, and in the COST well is represented by an interval of chert. This

unit is predominately **calcareous** shale and **siltstone** with interbeds of sandstone. **McCulloch** and others (1979) suggest that this unit may be partly equivalent to the **Sisquoc** Formation of late Miocene to early Pliocene age in the Santa Maria Basin.

Geologic Structure

The most significant structural features in the Point Conception area are low-angle reverse or thrust faults (pi. 15). These faults generally trend northwest **in** the northwestern part of the region, swinging to a westerly orientation in the southeast part. Three or more major thrust sheets or nappes are defined by these faults. The complexity **of surficial** and subsurface structure varies significantly between these **nappes**.

The small, **westward** thrust nappe in the northwestern part of the study area contains the most **severly** deformed (folded and faulted) sediments in the region. The western boundary of the nappe is composed of several thrust faults that dip eastward. These faults merge to form a single, major, through-going fault to the southeast. This major fault lies just east of, and parallel to a flat surfaced basement high that joins the Santa Lucia Bank to the north with the Channel Islands platform to the south. At its southeastern end, near Point Conception, it trends almost east. This thrust fault is seen in the seismic reflection profiles as a curving fault plane, convex to the east, that offsets late Pliocene sedimentary rocks. It displaces the base of acoustic unit C, and extends **upward** into the sedimentary sequence compressing this unit into an **anticlinal** fold.

Near the western margin of this **nappe**, northwest-trending **anticlines** and **synclines** that are parallel or sub-parallel to the bounding thrust fault are concentrated within unit C and the older sedimentary rocks of the nappe. West

of this bounding thrust **fault**, Pliocene and older sedimentary rocks caught between the nappe and the basement high are also faulted and folded.

Five heads of **Arguello** Canyon cut across this nappe; all of these are constructional canyons with well developed levees. These levees are mainly restricted to the nappe and do not extend onto the shelf to the east or, with the exception of perhaps one, across the western boundary faults. Only one other leveed canyon head is found in this region, and this is located southwest of Point Conception.

The largest nappe in the study area is bounded on the **west** by a major through-going thrust fault that parallels the basement high just north west of the Channel Islands platform. Except for minor faults and folds, this nappe has little superimposed structure. The frontal thrust fault displaces late Pliocene sediments (unit C) in the west, and Quaternary sediments (both units A and B) in the east. In the seismic reflection records the fault appears as a gently eastward-dipping plane associated with normal faulting and contorted bedding in the vicinity of the thrust (fig. 5). Two high-angle reverse or normal faults appear to continue uninterrupted along an easterly trend for over 20 km near the shelf break just offshore from the coastline immediately southeast of Point Conception. These faults are parallel or **subparallel** to the frontal thrust of the nappe and are downthrown to the north; locally they offset the sea **floor**. Short, discontinuous folds on the shelf north of these faults appear to parallel the trend of the faults.

The third nappe is located between the other **two** thrust sheets, just offshore between Point **Arguello** and Point Conception. This nappe has a nearly east-trending thrust fault boundary that joins the thrust forming the southern boundary of the nappe to the north. The thrust fault offsets sedimentary rocks of late Pliocene age (unit C). With the exception of a few discon-

tinuous faults and folds, this mppe has little superimposed structure. However, several fairly continuous, northwest-trending folds and faults disrupt late Pliocene to early Pleistocene sediments on the shelf landward (northeast) of the nappe. Near the shelf break, a northwest-trending normal or high angle reverse fault, downdropped to the south, offsets the sea floor and appears to truncate the bounding thrust faults of the central and northern nappes.

A Pleistocene angular unconformity that is well defined in the seismic reflection profiles crops out on the sea floor near the **scarp** marking the shelf edge at a 100 m depth (pi. 17). This feature extends from the northern part of the study area around Point Conception to the southeast. The outcrop of this unconformity is fairly continuous, but it is locally dislocated by faults mapped near the shelf break.

Bedrock crops out on the shelf in the vicinity of Point **Arguello** and Point Conception, as well as in the western part of the shelf that extends eastward from Point Conception. Bedrock **is** not exposed on the slope, except locally near the 100 m **scarp**. The north slope of Santa Barbara basin and the adjacent continental slope are covered with Quaternary sediment, much of which is slowly moving downslope.

Structure of the Point Conception region suggests that the area has undergone east-west compression. At least three imbricate thrust sheets or nappes were pushed **westward** during late Pliocene time. Sea-floor displacement along some conjugate faults and possible offset of Quaternary sediments (units A and B) suggest that thrusting of these nappes may continue today. Compressive forces associated with strike slip along the San Andreas fault appear to have resulted in decoupling of late Tertiary bedrock from older basement rocks. The basement high that joins the Santa Lucia Bank and Channel

Islands platform appears to have acted as a resistant barrier against which younger rocks were upthrust.

The most northerly of the three **nappes** appears to have undergone the greatest compression, as late Neogene sediments within the thrust sheet are more extensively folded and faulted than *in* any of the other **nappes**. Strata immediately **west** of the bounding thrust, in front of the **nappe**, have been compressed against the basement high and faulted at low angles from the westward thrusting (pi. 15).

The presence of leveed submarine canyons on the surface of the nappe suggests uplift in the adjacent region. Constructional (leveed) submarine canyons are uncommon in the shallow waters of the upper slope, and characteristically occur near the base of the continental slope or rise, or on the flat ocean floor where sediment laden currents lose energy. However, in this area it appears probable that during Pleistocene time a heavily sediment laden river debouched on the flat coastal plain in the present area of this **nappe**, where the levees were constructed from overbank flow during times of flooding.

The other two nappes within the study area are much less deformed than is the nappe described above. The lack of complex superimposed structure on these **two** nappes suggests that **compressional** forces were not as great here as farther north, or that thrusting was initiated in the north so that the more northerly mpppe has undergone thrusting for a longer time.

The evidence from seismic reflection records studied for this report largely reflects late Tertiary tectonic activity. However, deep-penetration, CDP multi-channel seismic reflection records from this area show evidence of early Tertiary thrusting as well (D. S. **McCulloch**, personal **commun.** , 1979). Lower to middle Tertiary sedimentary rocks were decoupled from older basement

and thrust westward against a basement high on the outer shelf during a period of east-west compression. The area immediately south of Point Conception is located on the largest and most southerly nappe mapped in the region. Structures superimposed on this **nappe** along the outer slope are relatively simple; however, structures on the shelf are more complex, suggesting that compressive forces may be active there today. A south-dipping thrust fault trends parallel to the coastline in this area and appears to disrupt Quaternary sediments that cover the outer shelf. Also, a fairly continuous fault appears to have controlled the development of the shelf break in this region. Side-scan sonographs and high-resolution seismic reflection profiles suggest that channels incised into the shelf are structurally controlled by faults. Consequently, we believe that the shelf and slope **physiography** and geology in the general vicinity of Point Conception reflect the same dynamic tectonic processes that have formed the major thrust sheets and **compressional** structures in the Santa Ynez Mountains.

Seismicity

The distribution of instrumentally recorded (post-1932) **seismicity** in the Santa Barbara Channel region is well characterized by the 1970 - 1975 instrumental record relocated and analyzed by Lee and others (1979). That study shows that post-1970 seismicity in the study area is relatively sparse. Epicenters and hypocenters west of **120°30'W** and north of **34°45'N** are poorly located because of an **inadequate** network coverage. East and south of these boundaries well-located earthquakes and well constrained fault-plane solutions can be associated geometrically with specific east-trending reverse faults such as Mid-channel, Pitas Point-Ventura, Red Mountain, and **Anacapa** faults (Yerkes and others, 1980). These faults show fairly uniform steeply

north-dipping slip vectors in contrast to the few semi-constrained solutions for the area to the west, **which** indicate gently east-plunging slip vectors.

Two large historic earthquakes have occurred in the general western Santa Barbara channel region. One event, located somewhere in the western Transverse Ranges, occurred December 21, 1812 and had an estimated magnitude of 7 to 7.5. The other was a M7.3 **temblor** that occurred November 4, 1927 along or near the **Arguello-North** Channel slope (Yerkes and others, 1980).

Both epicenters are poorly located. The 1927 earthquake has been intensively studied in recent years because of its relevance to coastal deformation northwest of Point **Arguello**. Three alternative locations for the 1927 event and **two** alternate locations for the 1812 event are shown on Plate 18; one other alternate location for the 1812 event is located off the map, due east of the study area in the central part of the Santa Barbara Channel (**Yerkes** and others, 1980, Sheet **1**).

Relatively little **is** known about the earthquake of 1812, which consisted of 2 large magnitude events that occurred within 30 minutes of each other, and severely damaged mission structures at San Fernando, San Buenaventura (Ventura), Santa Barbara, Santa Ynez, and **Purisima** (near **Lompoc**). Yerkes and others (1980) state that a moderate tsunami was associated with the earthquakes indicating that the events were centered somewhere in the Santa Barbara Channel and that dip slip or **landsliding** occurred at the sea floor.

Little more is known about the location of the 1927 epicenter. However, investigators have recently concluded that the epicenter was much closer to shore, 25 km or less, than the originally estimated distance of 80 km (**Gawthrop**, 1978a; Smith, 1978; Hanks, 1979). A seismic sea wave was reported to have been associated with this earthquake as well (Wood and others, 1966, p. 34). The presence of a tsunami indicates that dip slip or submarine

landsliding occurred on the sea floor. **Teleseismic** first-motion data and **analysis of** distortion of a large geodetic quadrilateral on the coastal mainland are consistent with thrust faulting, rather than strike slip on a northwest-trending fault such as the offshore **Lompoc** fault (Hanks, 1979; Savage and Prescott, **1978**; Yerkes and others, 1980, sheet 1). This reverse fault displays evidence of more than 152 m of Holocene displacement and is associated with deformation of the sea floor (**Yerkes** and others, 1980).

The distribution of epicenters both onshore and offshore is random and generally shows little or no preferred orientation or correlation with mapped faults (pl. 18). This is most likely the result of poor coverage by the seismographic **network** in this region. However, several clusters of epicenters occur in significant locations. Epicenters are concentrated along a fairly large area on the Santa Lucia Bank in the northwest part of the study area (pl. 18). Although no faults are shown in this area, perhaps because of the paucity of marine geophysical data there, these events may be associated with deep faulting within the bedrock ridge.

Another smaller, tightly spaced cluster of epicenters is located on the nearshore shelf immediately west of Point Conception. These events appear to be associated with Holocene faulting that is active on the shelf. A **first-** motion solution (G-n, **pl. 18**) for one of the events indicates an inferred westward thrusting on an eastward-plunging slip vector (**Gawthrop, 1978b**). **Two** other fault-plane solutions in the western Santa Barbara channel indicate active thrust faulting. A solution calculated by Gawthrop (**1978b**) from a seismic event along the eastern edge of the bedrock ridge (G-17, pl. 18) also indicates an inferred eastward-plunging slip vector that was probably associated with **movement** along the fairly continuous thrust fault that bounds the bedrock ridge. The other solution is from an event that occurred along

the western flank of the Santa Barbara Basin and shows an inferred **north-** plunging slip vector (Lee and others, 1979). This event may have been associated with reverse movement along the Mid-channel fault (pi. **18**).

Seafloor Instability

Areas of potential sea floor instability usually are mapped by the identification of features thought to characterize **downslope** sediment creep and submarine slides and slumps on seismic reflection profiles. All of these types of **downslope** mass movement are present in the western Santa Barbara Channel-Point Conception offshore area (pi. 16). Another factor contributing to sea-floor instability is the potential for liquefaction of bottom sediments. However, at present, not enough is known concerning the engineering properties of sediments in the western Santa Barbara Channel region to assess their liquefaction potential.

A considerable amount of sediment has been deposited within the western Santa Barbara Basin and along the slope seaward of Point **Arguello** and Point Conception since middle Tertiary time. Unstable sea-floor conditions are generally restricted to these areas of relatively rapid sedimentation and they are characterized by the presence of slumps and landslides, probable **downslope** sediment creep, buried channels, and levees (**pls. 16** and 17).

Submarine Slumps, Slides and Sediment Creep. Several submarine slumps and slides are present within the headward tributaries of **Arguello** Canyon and along the lower boundaries of some areas of sediment creep (pi. 16). Submarine slides and slumps, including a buried slide, also are mapped by Yerkes and others (1980) as covering a large area along the south slope of the Santa Barbara Channel in the extreme eastern part of the study area (pi. 16). Moreover, folded and contorted bedding in the shallow subsurface

indicate that slope deposits **in** this area have been unstable throughout Pleistocene and Holocene time.

Sediment creep appears to **be** fairly widespread along the slope immediately offshore of Point **Arguello** and Point Conception (Pi. 16). This area of creep is closely associated with levees and buried channels that in turn reflect rapid sedimentation, probably during Pleistocene time. This history has created a large area that is characterized by relatively unstable sea-floor conditions.

Buried and Active Channels. Both shallowly and deeply buried channels are mapped within the area of probable sediment creep, along the Point **Arguello-Point** Conception slope (pi. 16). Many of these channels are directly beneath or are closely associated with present-day tributaries to **Arguello** Canyon. **These** features reflect a period of active erosion and deposition during Pleistocene time.

Modern sediment transported along the shelf and slope of the Point Conception region reaches the deep-sea floor principally through **Arguello** Canyon. In addition, tributaries to **Arguello** Canyon as well as other submarine channels carry sediment southward from the Santa Lucia Bank, westward from the Point Conception shelf and the western Santa Barbara sill, southward from the San Miguel and Santa Rosa Islands platform and from the area of Rodriguez **seamount** (pi. 16). These channels are identified principally from bathymetry and most are of minor significance as conduits of sediment transport. However, the five tributaries of **Arguello** Canyon that notch the distal edge of the shelf off Point Conception appear to be major sediment conduits, and probably most of the modern sediment carried across the shelf is swept into the **Arguello** Canyon system, in which it is then carried to the continental rise and abyssal plain.

Levees. Six well defined submarine-channel levees have been mapped on the upper slope west of Point Conception (pi. 16). Most of these are located due **west** of Point **Arguello** where they are associated with the active **tribu-**
taries to Arguello Canyon. These features probably were constructed by overbank flows of currents that were heavily laden with sediment during periods of rapid **downslope** transport, most likely during Pleistocene time. These levees are found unusually high on the continental slope, as levees are generally found near the base of the slope or rise where sediment-laden currents lose energy. As noted previously, the presence of levees on the upper slope may reflect the tectonic elevation of features that were constructed at greater depths.

The relative lack of consolidation and fine grain size of the sediment characteristic of levees, and the relatively steep slopes underlying levees in this area suggest that they may be potentially unstable. Water-saturated fine sand and silt in such levees, especially when situated in a tectonically active region such as the Point Conception area, probably are prone to liquefaction and their engineering properties should be carefully studied before any statement is made concerning their stability.

Unconsolidated sediment. An isopach map of unconsolidated shelf deposits inferred to be Quaternary in age was constructed from high-resolution **Uniboom** and 3.5 kHz seismic reflection profiles collected for this investigation (pi. 17). This map is limited to areas on the continental shelf where an unconformity of Pleistocene age made the correlation of younger deposits possible. This unconformity could not be identified on the adjacent slope, and Quaternary sediments could not be identified and correlated with confidence. The thickness of Quaternary sediment on the continental shelf varies from zero near the shelf break and along bedrock outcrops in the

vicinity of Point Conception to more than 15 meters. Quaternary deposits are thickest beneath the shallow shelf area between Point **Arguello** and **Purissima** Point.

Hydrocarbon Seepage and Shallow Gas Accumulations

Two areas of possible offshore oil **or** gas seepage are identified and mapped; one area is southwest of Point Conception and the other is west and northwest of Point **Arguello** (pi. 16). These seeps are restricted to the nearshore shelf **where** Tertiary bedrock is fractured by many short, discontinuous faults, some of which displace Pleistocene and Holocene sediment.

Bedrock Geology

Most of the Point Conception study area is covered by undifferentiated Quaternary and late Tertiary sediments (pi. 15). Bedrock crops out in two locations; one along the nearshore shelf just east of Point **Arguello** and continuing eastward around Point Conception to the eastern limit of the study area, and the other on the San Miguel Island platform (pi. 15). These rocks have been planed by erosion since Pleistocene time, and today most Holocene sediment carried to the shelf in this area is swept from this bedrock surface and deposited beyond the shelf break,

Miocene sedimentary rock (Monterey Formation?) is the principal bedrock type that crops out on the Point Conception shelf. In this area Miocene sedimentary rocks are folded and faulted and have a easterly structural trend. The wave-planed bedrock platform that surrounds San Miguel Island is composed of a core of Paleocene and Eocene sedimentary rock unconformably overlain by Miocene sedimentary rock (pi. 15). Similar to the exposed bedrock off Point Conception, these rocks are folded and faulted and exhibit a general easterly structural trend.

Extending **northwestward** from the western end of the Channel Islands platform is a shallowly buried subsurface bedrock and basement ridge that appears to connect the Channel Islands platform with Santa Lucia Bank (pi. 15). This ridge may consist of Franciscan basement rock overlain by early to middle Tertiary sedimentary rock that is in turn covered with a relatively thin veneer of Quaternary-Tertiary (undifferentiated) sediment. Complex folds and faults bisect this ridge in the vicinity of **Arguello** submarine canyon, possibly the result of tectonic bending.

Miocene (?) volcanic rocks form Rodriguez Seamount, located approximately 50 km **west** of San Miguel Island, and appear to be exposed on the sea floor in an area that lies along an east-west line between San Miguel Island and Rodriguez Seamount (pi. 15). Volcanic rocks of Miocene age also crop out on San Miguel Island and on the seafloor around the east end of the island. These volcanic rocks are aligned in an east-west direction and may connect at depth to a common volcanic ridge that underlies the Channel Islands platform.

Summary of Hazards

The most significant geologic hazard **identified** in the western Santa Barbara Channel-Point Conception area is seafloor instability. **High-** resolution seismic reflection data indicate that the upper slope offshore of Point **Arguello** and Point Conception is probably the site of active downslope **sediment** creep. Many tributaries to **Arguello** submarine canyon dissect this area, and submarine levee deposits, slumps, and incipient slumps indicative of unstable seafloor conditions are present.

Faults and earthquakes are also hazards of significance. Seismic reflection data collected from the Point Conception region show that faulting is extensive. Many faults are reverse or thrust faults, and displacements of

the seafloor and of Quaternary sediment indicate that many faults are active. Recent faulting, **along** with historical records of major earthquakes in the region, indicate that the western Santa Barbara Channel is tectonically active and could be the site of severe seismic events in the future.

Additional data are required for a comprehensive assessment of potential geological hazards in the western Santa Barbara channel region. In particular, data gaps exist concerning **seismicity**, hydrocarbon seepage, the liquefaction potential of unconsolidated sediment, and the tsunami hazard related to **seismicity** in this area.

- Agnew, D. C., 1979, Tsunami history of San Diego, in Abbott, **P.L.** and **W.J. Elliott, eds.**, Earthquakes and other **perils**, San Diego region: San Diego Association of Geologists Guidebook, pp. 117-122.
- Agnew, **D.C.**, M. **Legg**, and C. Strand, 1979, Earthquake history of San Diego, in Abbott, **P.L.** and **W.J.Elliott, eds.**, Earthquakes and other perils, San Diego region: San Diego Association of Geologists Guidebook, p. 123-138.
- **Arnal, R.E.** 1976, Miocene paleobathymetric changes of the Santa **Rosa-Cortes** Ridge area, California continental borderland, in Howell, D.G., cd., Aspects of the geologic history of the **California** continental borderland: American Association of Petroleum Geologists, Pacific Section, Miscellaneous Publication 24, p. 60-79.
- Bandy, O.L., **J.C. Ingle**, and **J.M. Resig**, 1964, **Facies** trends, San Pedro Bay, California: Geological Society of America Bulletin, v. 75, p. 403-424.
- Barnes, P.W., 1970, Marine geology and oceanography of Santa Cruz basin off southern California: University of Southern California, Department of Geological Sciences Report **USC-GEOL** 70-3, 175 pp.
- Barrows, A.G., 1974, A review of the geology and earthquake history of the Newport-Inglewood structural zone, southern California: California Division of Mines and Geology Special Report 114, 155 pp.
- Blanc, **R.P.** and **G.B. Cleveland**, 1968, Natural slope stability as related to geology, San **Clemente** area, Orange and San Diego Counties, California: California Division of Mines and Geology Special Report 98, 19 pp.
- **Clements**, T. and **K.O. Emery**, 1947, Seismic activity and topography of the sea floor off southern California: Seismological Society of America Bulletin, v. 3?, p. 309-313.
- **Coffman, J.L.** and **C.A. von Hake**, 1973, Earthquake history of the United States: National Oceanic and Atmospheric Administration Publication 41-1, Washington, 208 pp.
- Cole, M.R., 1970, **Paleocurrent** and basin analyses on San **Nicolas** Island, California: Ohio University unpublished Masters Thesis, 110 pp.
- Cole, M.R., 1977, Eocene **paleocurrents** and sedimentation, San **Nicolas** Island, California: American Association of Petroleum Geologists Bulletin, v. 61, no. 2, p. 237-247.
- Cook, N.E., editor, 1979, Geologic studies of the Point Conception deep stratigraphic test well **OCS-CAL** 78-164 No. **1**, outer continental shelf, southern California, United States: U.S. Geological Survey Open-File Report 79-1218, 148 pp.
- Dames & Moore, 1978, Preliminary **geotechnical** investigation offshore, beach, and **seacliff** areas--proposed LNG marine Terminal Point Conception, California--report for Western LNG Terminal Associates: Los Angeles, California, Dames & Moore, Job Nos. 0011-207-02 and 0011-209-02

- Dott, R. G., Jr. , 1963, Dynamics of subaqueous gravity **depositional** processes: American Association of Petroleum Geologists Bulletin, v. 47, no. 1, p. 104-128.
- Edgington, W.G., 1974, Geology of the Dana Point Quadrangle, Orange County, California: California Division of Mines and Geology Special Report 109, 31 pp.
- Edwards, B.D., **M.E. Field**, and **E.C. Clukey**, 1980, Geological and **geotechnical** analyses of a submarine slump, California borderland: Proceedings of the 12th Annual Offshore Technology Conference, Houston, Texas, paper no. OTC 3726, p. 399-410.
- Emery, K.O., 1952, Continental shelf sediments of southern California: Geological Society of America Bulletin, v. 63, p. 1105-1108.
- Emery, **K.O.** 1960, Basin plains **and** aprons off southern California: Journal of Geology, v. 68, p. 464-479.
- Emery, **K.O.** and D. **Hoggan**, 1958, Gases in marine sediments: American Association of Petroleum Geologists Bulletin, v. 42, no. 9, p. 2174-2188.
- Emery, **K.O.** and **S.C. Rittenberg**, 1952, Early diagenesis of California basin sediments in relation to origin of oil: American Association of Petroleum Geologists Bulletin, v. 36, p. 735-806.
- Field, **M.E.** and **S.H. Clarke**, Jr., 1979, Small-scale slumps and slides and their significance for basin slope processes, southern California borderland, in Doyle, **L.J.** and **O.H. Pilkey**, editors, Geology of continental slopes: Society of Economic Paleontologists and Mineralogists Special Publication 27, p. 223-230
- Field, **M.E.** and **B.D. Edwards**, 1980, Slopes of the southern California continental borderland: a regime of mass transport, in Field, **M.E.**, **A.H. Bouma**, **I.P. Colburn**, **R.G. Douglas**, and **J.C. Ingle**, editors, Quaternary depositional environments of the Pacific Coast: Society of Economic Paleontologists and Mineralogists, Pacific Section, Pacific Coast **Paleogeography** Symposium 4, Los Angeles, California, p. 169-184.
- Field, **M.E.** and **W.C. Richmond**, 1980, Sedimentary and structural patterns on northern Santa **Rosa-Cortes** Ridge, southern California: Marine Geology, v. 34, p. 79.
- Friedman, M.E., **J.H. Whitcomb**, **C.R. Allen**, and **J.A. Hileman**, 1976, Seismicity of the southern California region, 1 January 1972 to 31 December 1974: California Institute of Technology, Division of Geological and Planetary Sciences Contribution 2734, 404 pp.
- Gawthrop**, W.H., 1975, **Seismicity** of the central California coastal region: U.S. Geological Survey Open File report 75-134, 87 p.
- Gawthrop**, W.H., 1978a, The 1927 Lompoc California earthquake: Seismological Society of America Bulletin, v. 68, p. 1705-1716.

- Gawthrop, W. H., 1978b**, Seismicity and tectonics of the central California coastal region, in Silver, **E.A.** and **Normark, W.R., editors**, San **Gregorio-Hosgri fault zone**, California: California Division of Mines and Geology Special Report 137, p. 45-56.
- Gorsline, D.S., 1980**, **Sedimentologic** history and characteristics of continental margin **basins**, California borderland: American Association of Petroleum Geologists Bulletin, v. 64, p. 442-443.
- Gorsline, D.S. and D.J. Grant, 1972**, Sediment textural patterns on San Pedro shelf, California (1951-1971) , in Swift, **D.J.P.** , **D.P. Duane**, and **O.H. Pilkey**, editors, Shelf sediment transport: Dowden, **Hutchinson** and Ross, Inc., **Stroudsburg**, Pennsylvania, p. 575-600.
- Greene, H.G., **W.H.K. Lee**, **D.S. McCulloch**, and **E.E. Bragge**, 1973, Faults and earthquakes in the Monterey Bay region, California: U.S. Geological Survey Miscellaneous Field Investigation Map **MF-518**.
- Greene, H.G., **S.H. Clarke, Jr.**, **M.E. Field**, **F.I. Linker**, and **H.C. Wagner**, 1975, Preliminary report on the environmental geology of selected areas of the southern California continental borderland: U.S. Geological Survey Open-File Report 75-596, 69 pp.
- Greene, H.G., **S.C. Wolf**, and **K.G. Blom**, 1978, The marine geology of the eastern Santa Barbara Channel with particular emphasis on the **ground-water** basins offshore from the Oxnard Plain, southern California: U.S. Geological Survey Open-File Report 78-305, 104 pp.
- Greene, H.G., **S.H. Clarke, Jr.**, and **M.E. Field**, 1979, Environmental geology of the southern California borderland: U.S. Geological Survey Professional Paper 1150, p. 147.
- Gutenberg, B., 1943**, Earthquakes and structure in southern California: Geological Society of America Bulletin* **v. 54, no. 4**, p. 499-526.
- Hall, **R.W.** and **H.R. Enslinger**, editors, 1979, Potential geologic hazards and constraints for blocks in proposed mid-Atlantic OCS oil and gas lease sale 49: U.S. Geological Survey Open-File Report 79-264.
- Hampton, **M.A.** and **A.H. Bouma**, 1977, Slope instability near the shelf **break**, western Gulf of Alaska: Marine **Geotechnology**, v.2, p. 309-322.
- Hanks, T.C., 1979, The **Lompoc**, California earthquake (November 4, 1927; **M=7.3**) and its aftershocks: Seismological Society of America Bulletin, v. 69, **no.2**, p. 451-462.
- Harding, T.P., 1973, Newport-Inglewood trend, California - an example of wrenching style **of** deformation: American Association of Petroleum Geologists Bulletin, v. **57**, no. 1, p. 97-116.
- Heezen, B.C. and **C.L. Drake**, 1964, Grand Banks slump: American Association of Petroleum Geologists Bulletin, v. 48, p. 221-225.

- Henry, M. V., 1976, The unconsolidated sediment distribution on the San Diego County mainland shelf, California: San Diego State University unpublished Masters Thesis.
- Hileman, J.A.**, 1979, **Seismicity** of the San Diego region, in Abbott, **P.L.** and **W.J. Elliott**, editors, Earthquakes and other perils, San Diego Region: San Diego Association of Geologists Guidebook, p. 11-20.
- Hileman, J.A.**, **C.R. Allen**, and **J.M. Nordquist**, 1973, **Seismicity** of the southern California region, 1 January 1932 to 31 December 1972: California Institute of Technology, Division of Geology and Planetary Sciences Contribution **number 2385, 404 pp.**
- Howell, D.G., **C.J. Stuart**, **J.P. Platt**, and **D.J. Hill**, 1974, Possible **strike-slip** faulting in the southern California borderland: *Geology*, v* 2, p. 93-98.
- Jennings, C.W., 1973, State of California **preliminary** fault and geologic map: California Division of Mines and Geology preliminary report 13.
- Jennings, **C.W.** 1977, Geologic map of California: California Geologic Data Map Series, California Division of Mines and Geology, scale **1:750,000.**
- Kennedy, M.P., 1975, Geology of the San Diego metropolitan area, California Division of Mines and Geology, Bulletin 200, p. 1-39.
- Kennedy, M.P., **E.E. Welday**, **G. Borchardt**, **T.W. Chase**, and **R.H. Chapman**, 1977, Studies on surface faulting and liquefaction as potential earthquake hazards in urban San Diego, California: California Division of Mines and Geology final technical report submitted to U.S. Geological Survey (USGS Contract number 14-08-0001-15858, 52 pp.
- Lee, **W.H.K.** and **J.G. Vedder**, 1973, Recent earthquake activity in the Santa Barbara Channel region: *Seismological Society of America Bulletin*, v. 63, p. 1757-1773.
- Lee, W.H.K., **R.F. Yerkes**, and **M. Simirenko**, 1979, Recent earthquake activity and focal mechanisms in the western Transverse Ranges, California: U.S. Geological Survey Circular 799-A, 37 pp.
- Legg, Mark and **D.C. Agnew**, 1979, The 1862 earthquake in San Diego, in Abbott, **P.L.** and **W.J. Elliott**, editors, Earthquake and other perils, San Diego region: San Diego Association of Geologists Guidebook, p. 139-142.
- Legg**, Mark and **M.P. Kennedy**, 1979, Faulting offshore San Diego and northern Baja California, in Abbott, **P.L.** and **W.J. Elliott**, editors, Earthquakes and other perils, San Diego Region: Geological Society of America Annual Meeting Guidebook, p. 29-46.
- Lewis, K.B., 1971, Slumping on a continental slope inclined at 1°-40: *Sedimentology*, v. 16, p. 97-110.

- Marine Environmental Science Associates and Marine Studies, Geosciences Department California State University (MESA, Inc.), Northridge, 1978, A geophysical and geologic evaluation of the offshore extension of the Santa Ynez fault, South branch, northwestern shelf of the Santa **Barbara** basin (between San Augustine and **Alegria** Creek): report prepared for Dames & Moore, Los Angeles, 19 pp., 5 plates
- McCulloch, D.S., J.G. Vedder, H.C. Wagner, and R.H. Brune**, 1979, Geologic setting, in Cook, **H.E.**, editor, Geologic studies of the Point Conception deep **stratigraphic** test well **OCS-CAL** 78-164 No. 1 Outer Continental Shelf southern California, United States: U.S. Geological Survey Open-File Report 79-1218, p. 10-25.
- Menard, H.W., R.F. Dill, E.L. Hamilton, D.G. Moore, G. Shumway, M. Silverman, and H.B. Stewart**, 1954, Underwater mapping by diving geologists: American Association of Petroleum Geologists Bulletin, v. 38, p. 129-147.
- Mikolaj, P.G., R.S. Schlueter, and A.A. Allen**, 1972, Investigation of the nature, extent, and fate of **natural** oil seepage off southern California: Fourth Annual Offshore Technology Conference, Houston, Texas, v. 1, p. 365-380.
- Miller, **R.V.** and S.S. Tan, 1976, Geology and engineering geologic aspects of the south half Tusten Quadrangle, Orange County, California: California Division of Mines and Geology Special Report 126, 28 pp.
- Moody, J.D., **and M.J. Hill**, 1956, Wrench fault tectonics: Geological Society of America Bulletin, v. 67, p. 1207-1246.
- Moore, D.G., 1954, Submarine geology of San Pedro Shelf: Journal of Sedimentary Petrology, v. 24, p. 162-181.
- Moore, D.G., 1960, Acoustic reflection studies **of** the continental shelf **and** slope off southern California: Geological Society of America Bulletin, v. 71, p* 1121-1136.
- Moore, D.G., **1961**, Submarine slumps: **Journal** of Sedimentary Petrology, v. 31, p. 343-357.
- Moore, D.G., 1969, Reflection profiling studies of the California continental borderland: Structure and Quaternary turbidite basins, Geological Society of America Special Paper 107, 142 pp.
- Morton, P.K., 1974, Geology and engineering geologic aspects of the south half of the Gobernadora Quadrangle, Orange County, California: California Division of Mines and Geology Special Report 111, 30 pp.
- Morton, P.K., **R.V. Miller, and D.L. Fife**, **1973**, Preliminary gee-environmental maps of Orange County, California: California Division of Mines **and** Geology Preliminary Report 15, 4 plates.

- Morton, P. K., **W.J. Edgington**, and **D.L. Fife**, 1974, Geology and engineering geologic aspects of the San Juan Capistrano Quadrangle, Orange County, California: California Division of Mines and Geology Special Report 112, 64 pp.
- Nelson, C.H., **K.A. Kvenvolden**, and **E.C. Clukey**, 1978, **Thermogenic** gases in near surface sediments of Norton Sound, Alaska, in Proceedings of the 10th Annual Offshore Technology Conference, **Houston**, Texas, paper number OTC 3354, p. 2623-2633.
- Norris, R.M., 1951, Marine geology of the San **Nicolas** Island region, California: Scripps Institution of Oceanography unpublished Doctoral Thesis.
- Orr, **W.L.** and **K.O. Emery**, 1956, Composition of organic matter in marine sediments--preliminary data on hydrocarbon distribution in basins off southern **California**: Geological Society of America Bulletin, v. 67, p. 1247-1258.
- Payton, C.E., editor, Seismic **stratigraphy**--applications to hydrocarbon exploration: American Association of Petroleum Geologists, Memoir 26, 516 pp.
- Real, C.R., **T.R. Toppazada**, and **D.L. Parke**, 1978, Earthquake catalog of California--January 1, 1900 to December 31, 1974: California Division of Mines and Geology Special Publication 52, **15pp.**
- Richmond, W.C., **L.J. Cummings**, **S. Hamlin**, and **M.E. Nagaty**, 1981, Geological hazards and constraints in the area of proposed OCS oil and gas lease sale 48, southern California: U.S. Geological Survey Open-File Report 81-307.
- Richter, C.F., 1958, Elementary seismology: San Francisco, **W.H. Freeman**, 768p.
- Savage, **J.C.** and **W.H. Prescott**, 1978, Geodetic control and the 1927 **Lompoc**, California earthquake: Seismological Society of America Bulletin, v. 68, no. 6, p. 1699-1703.
- Smith, S.W., 1978, Sea floor expression of the 1927 **Lompoc** earthquake abstract: EOS, American Geophysical Union Transactions, v. 59, no. 12, p. 1128.
- Stevenson, R.E., **E. Uchupi**, and **D.S. Gorsline**, 1959, Some characteristics of sediments on the mainland shelf of southern California in Oceanographic survey of the continental shelf area of southern California: California State Water Pollution Control Board Publication 20, p. 59-109.
- Tan, S.S. and **W.J. Edgington**, 1976, Geology and engineering geologic aspects of the **Laguna** Beach Quadrangle, Orange County, California: California Division of Mines and Geology Special Report 127, 32pp.

- Topozada, T. R., Real, C. R., Bezore, S. P., and Parke, D. L., 1979, Compilation of pre-1900 California earthquake history: California Division of Mines and Geology **Open-File** report OFR 79-6, SAC, 271p.**
- Townley, S.D. and M.W. Allen, 1939, Descriptive catalog of earthquakes of the Pacific coast of the United States, 1769-1928: Seismological Society of America Bulletin, v. 29, p. 1-297.**
- Uchupi, E., 1961, Submarine geology of the Santa Rosa-Cortes Ridge: Journal of Sedimentology and Petrology, v. 31, p. 534-545.**
- Uchupi, E. and R.A.P. Gaal, 1963, Sediments of the Pales Verdes shelf, in Clements, T., editor, Essays in marine geology in honor of K.O. Emery: Southern California University Press, p. 171-189.**
- Van Dorn, W.G., 1979, Theoretical aspects of tsunamis along the San Diego coastline, in Abbott, P.L. and W.J. Elliott, editors, Earthquake and other perils, San Diego region: Geological Society of America Annual Meeting guidebook, p. 115-116.
- Vedder, J.G., 1976, Precursors and evolution of the name California continental borderland, in Howell, D.G., editor, Aspects of the geologic history of the **California continental** borderland: American Association of Petroleum Geologists, Pacific Section, Miscellaneous Publication 24, p. 6-11.
- Vedder, J.G. and R.M. Norris, 1963, Geology of San **Nicolas** Island, California: U.S. Geological Survey Professional Paper 369, 65 pp.
- Vedder, J.G., L.A. Beyer, Arne Junger, C.W. Moore, A.E. Roberts, J.C. Taylor, and H.C. Wagner, 1974, Preliminary report on the geology of the continental borderland of southern California: U.S. Geological Survey Miscellaneous Field Studies Map MF-624, 34 pp.**
- Vedder, J.G., J.K. Crouch, E.W. Scott, H.G. Greene, D. Cramer, M. Ibrahim, R.B. Tudor, and G. Vinning, 1980, A summary report of the regional geology, petroleum potential, environmental geology, and operational considerations in the area of proposed lease sale no. 68, offshore southern California: U.S. Geological Survey Open-File Report 80-198, 62 pp.
- Weaver, D.W. and D.P. Doerner, 1969, Structural setting, northern Channel Islands, southern California borderland, in Weaver, D.W., D.P. Doerner, and B. Nolf, Geology of the northern Channel Islands, Pacific Sections, American Association of Petroleum Geologists and Society of Economic Paleontologists and Mineralogists Special Publication, figure 14.
- Welday, E.E. and J.W. Williams, 1975, Offshore surficial geology of California: California Division of Mines and Geology Map Sheet 26.**
- Wentworth, C.M., J.I. Ziony, and J.M. Buchanan, 1970, Preliminary geologic environmental map of the greater Los Angeles area, California: U.S. Geological Survey report, TID 25363, 41 pp.**

- Wilcox, R. E., **T.P. Harding**, and **D.R. Seely**, 1973, Basic wrench tectonics: American Association of Petroleum Geologists, v. 57, p. 74-96.
- Wilkinson, G.R., 1971, California offshore oil and gas seeps: California Division Oil and Gas Summary of Operations, v. 57, no. 1, p. 5-28.
- Wimberley**, C.S., 1964, Sediments of the southern California mainland shelf: University of Southern California unpublished doctoral thesis.
- Wolf**, S.C., 1975, Seismic reflection profiles, R/V POLARIS, March 1972, offshore southern California, Point Conception cruise: U.S. Geological Survey Open-File Report 75-166, 22 pp.
- Wood, H.O., **N.H. Heck**, and **R.A. Eppley**, 1966, Earthquake history of the United States, Part II, Stronger earthquakes of California and western Nevada: U.S. Department of Commerce, Environmental Science Services Administration, Coast and Geodetic Survey, No. 41-1, revised.
- Yerkes, R.F., **H.G. Greene**, **J.C. Tinsley**, and **R.K. Lajoie**, 1980, Seismotectonic setting of the Santa Barbara channel area, southern California: U.S. Geological Survey **MF-1169**, 1 plate with text, 10 pp.
- Ziony**, J.I., **C.M. Wentworth**, **J.M. Buchanan-Banks**, and **H.C. Wagner**, 1974, Preliminary map showing recency of faulting in coastal southern California: U.S. Geological Survey Miscellaneous Field Studies Map **MF-585**.

APPENDIX 1: Location, Depth, Length and Type of Selected Samples from the Southern California
Continental Borderland

Sta	Sample	Sample	Location	1978		Water Depth(m)	Sample Length(m)
				Latitude	Longitude		
01	01D2	Dart Core	San Pedro Shelf	+33° 36.6'	-118° 11.6'	45	Smear slide only
02	02D1	"	"	+33° 36.3'	-118° 01.12'	46	0.19
03	03D1	"	"	+33° 36.5'	-118° 02.2'	47	0.18
04	04D1	"	"	+33° 35.8'	-118° 10.9'	41	0.48
05	05D1	"	"	+33° 35.39'	-118° 11.5'	60	0.21
06	06D1	"	"	+33° 35.95'	-118° 09.40'	43	0.17
07	07D1	"	"	+33° 35.7'	-118° 08.7'	45	0.17
08	08D	"	"	+33° 35.35'	-118° 09.40'	45	0.53
09	09D1	"	"	+33° 33.01'	-118° 12.90'	253	0.40
10	10D1	"	"	+33° 32.5'	-118° 03.25'	275	0.54
11	11D1	"	"	+33° 35.89'	-118° 08.90'	45	0.17
12	12D1	"	"	+33° 35.38'	-118° 08.45'	49	0.18
13	13D1	"	"	+33° 35.47'	-118° 08.29'	50	0.185
14	14D1	"	"	+33° 39.65'	-118° 03.09'	15	0.16
15	15D1	"	"	+33° 39.36'	-118° 02.99'	15	Core Catcher only
16	16D1	"	"	+33° 39.15'	-118° 02.92'	17	0.21

Sta	Sample	Sample	Location	Latitude	Longitude	Water	Sample
17	17D1	Dart Core	Shelf off Dana Point	+33° 28.84'	-117° 57.03'	380	0.23
18	18G1	Gravity Core	"	+33° 14.8'	-117° 56.2'	645	1.95
19	19G1	"	"	+33° 20.3'	-117° 56.07'	579	1.51
20	20G1	"	"	+33° 19.5'	-117° 56.99'	655	1.73
21	21G1	"	"	+33° 21.47'	-117° 50.17'	639	1.52
22	22G1	"	"	+33° 21.47'	-117° 50.55'	622	1.90
23	23G1	"	San Diego Shelf	+33° 19.72'	-117° 37.73'	234	0.46
24	24G1	"	"	+33° 20.16'	-117° 36.70'	62	Core Catcher
25	25G1	"	"	+32° 41.21'	-117° 22.5'	290	1.25
26	26G2	"	"	+32° 41.25'	-117° 22.60'	303	1.40
27	27G1	"	"	+32° 43.3'	-117° 28.5'	530	2.15
28	28G1	"	"	+32° 43.6'	-117° 28.2'	543	2.08
29	29D1	Dart Core	"	+32° 46.9'	-117° 21.24'	7.8	0.155
30	30D1	"	"	+32° 50.8'	-117° 19.2'	393	0.45
31	31D1	"	"	+32° 50.05'	-117° 13.2'	57	0.255
32	32G1	Gravity Core	"	+32° 53.10'	-117° 17.80'	326	1.93
33	33G1	"	"	+32° 53.7'	-117° 17.75'	393	1.02
34	34G1	"	"	+32° 52.35'	-117° 20.08'	196	0.63

Sta	Sample Number	Sample Type	Location	Latitude	Longitude	Water Depth (m)	Sample Depth (m)
35	35G1	Gravity Core	San Diego Shelf	+32° 53.9'	-117° 24.95'	575	2.16
36	36G1	"	"	+32° 54.13'	-117° 24.67'	588	2.03
37	37G1	"	"	+32° 55.52'	-117° 21.47'	492	1.84
38	38D1	Dart Core	"	+32° 52.5'	-117° 21.05'	315	0.55
39	39D1	"	"	+32° 52.19'	-117° 21.7'	322	0.41
40	40D1	"	"	+32° 50.88'	-117° 22.47'	314	0.50
41	41D1	"	"	+32° 50.19'	-117° 23.44'	383	0.45
42	42D1	"	"	+32° 49.94'	-117° 23.8'	415	0.50
43	43D1	"	"	+32° 49.78'	-117° 24.04'	435	0.23
44	44D1	"	"	+32° 49.18'	-117° 24.78'	475	0.35
45	45G1	Gravity Core	"	+32° 48.91'	-117° 24.73'	495	1.68
46	46G1	"	San Nicolas Island	+33° 07.00'	-119° 33.10'	935	0.19
47	47G1	"	"	+33° 09.95'	-119° 30.05'	770	0.56
48	48G1	"	"	+33° 08.00'	-119° 30.80'	980	0.63
49	49G1	"	"	+33° 05.88'	-119° 32.71'	705	1.50
50	50G1	"	"	+33° 04.84'	-119° 33.11'	371	Core Catcher

Sta	Sample Number	Sample Type	Location	Latitude	Longitude	Water Depth (m)	Sample T (m)
<u>1979</u>							
51	51G1	Gravity Core	Gulf of Santa Catalina - Lasuen Knoll	+33° 21.64'	-117° 59.25'	719	1.8
51	51G2	"	"	+33° 21.64'	-117° 59.25'	686	1.97
52	52G	"	"	+33° 21.89'	-117° 58.77'	560	1.03
53	53G	"	"	+33° 24.43'	-118° 02.05'	555	1.46
54	54G	"	"	+33° 24.23'	-118° 02.47'	692	1.2
55	55G3	"	"	+33° 27.49'	-118° 03.24'	422	"small recovery"
56	56G	"	San Pedro Basin	+33° 29.59'	-118° 15.37'	847	1.8
57	57G	"	"	+33° 29.24'	-118° 15.27'	787	1.45
58	58G	"	San Pedro Shelf	+33° 39.93'	-118° 13.88'	022	0.36
59	59G1	"	"	+33° 38.74'	-118° 13.53'	022	0.46
59	59G2	"	"	+33° 39.62'	-118° 13.70'	022	c.c. only
60	60G	"	"	+33° 38.42'	-118° 13.53'	036	c.c. only
62	62G	"	"	+33° 37.99'	-118° 12.47'	035	0.44
63	63G	"	"	+33° 34.66'	-118° 08.43'	075	c.c. only
64	64G	"	"	+33° 35.04'	-118° 09.02'	058	c.c. only
65	65P	Piston Core	San Mateo Point	+33° 19.60'	-117° 43.50'	727	2.03
65	65G	Gravity Core	"	+33° 19.36'	-117° 43.78'	732	1.53

Sta	Sample Jumb	Sample	Location	Latitude	Longitude	Water Depth (m)	Sample Depth (m)
66	66G	Gravity Core	San Mateo	+33° 20.57'	-117° 42.58'	607	2.57
66	66P	Piston Core	" Point	+33° 20.55'	-117° 42.65'	617	≥.89
67	67P	"	"	+33° 20.57'	-117° 43.02'	662	2.78
67	67G	Gravity Core	"	+33° 20.62'	-117° 42.98'	656	2.41
68	68G1	"	"	+33° 19.02'	-117° 41.28'	642	2.47
68	68G2	"	"	+33° 18.92'	-117° 41.30'	633	2.24
69	69G1	"	"	+33° 17.88'	-117° 42.62'	738	2.34
69	69G2	"	"	+33° 17.61'	-117° 42.35'	730	2.37
69	69G3	"	"	+33° 17.82'	-117° 42.43'	733	2.57
70	70G2	"	"	+33° 17.70'	-117° 42.87'	754	0.94
71	71D1	Dart Core	Las Flores	+33° 16.83'	-117° 34.22'	071	0.20
71	71D2	"	" Shelf	+33° 16.83'	-117° 34.22'	072	0.30
72	72D	"	"	+33° 16.67'	-117° 34.12'	073	0.30
73	73D	"	"	+33° 16.66'	-117° 33.99'	070	0.30
74	74D	"	"	+33° 16.46'	-117° 33.86'	072	0.36
75	75G	Gravity Core	Gulf of Santa Catalina	+33° 06.87'	-117° 46.10'	827	1.85
76	76G	"	"	±33° 06.55'	-117° 46.09'	843	0.43
77	77G2	"	"	+33° 06.46'	-117° 45.78'	790	1.69

Sta	Sample Number	Sample Type	Location	Latitude	Longitude	Water Depth (m)	Sample Depth (m)
78	78G	Gravity Core	Gulf of Santa Catalina	+33° 06.05'	-117° 44.39'	762	1.80
79	79G	" "	" "	+33° 05.71'	-117° 45.55'	844	0.73
	80G	" "	" "	+33° 05.77'	-117° 45.33'	822	0.85
81	81G	" "	" "	+33° 04.60'	-117° 44.93'	850	0.69
82	82G	" "	" "	+33° 04.74'	-117° 44.34'	788	1.37
83	83G	" "	" "	+33° 04.89'	-117° 44.2°	730	1.25
84	84G	" "	" "	+33° 04.98'	-117° 43.82'	700	1.58
85	85G	" "	" "	+32° 58.16'	-117° 35.36'	731	1.68
	86G	" "	" "	+32° 58.06'	-117° 5.35'	747	1.61
87	87G	" "	" "	+32° 58.13'	-117° 35.25'	748	1.64
88	88G	" "	San Diego Trough	+32° 51.76'	-117° 43.20'	1070	1.85
89	89G	" "	" "	+32° 51.44'	-117° 43.22	1076	1.14
90	90P	Piston Core	" "	+32° 49.53'	-117° 41.53'	1065	0.34
90	90G	Gravity Core	" "	+32° 49.52'	-117° 41.51'	1066	2.30
91	91G1	" "	" "	+32° 49.22'	-117° 41.78'	1080	0.38
91	91G2	" "	" "	+32° 49.31'	-117° 41.77'	1080	0.40
92	92G	" "	Gulf of Santa Catalina	+32° 50.47'	-117° 31.28'	840	2.31
93	93G	" "	" "	+32° 50.28'	-117° 31.42'	845	2.48

Sta	Sample umb	Sample	Location	Latitude	Longitude	Water	Sample gt
94	94G	Gravity Core	Gulf of Santa Catalina	+32° 51.84'	-117° 28.45'	684	1.93
95	95G	" "	" "	+32° 51.50'	-117° 28.34'	679	2.33
96	96G	" "	Coronado Bank	+32° 43.02'	-117° 27.76'	640	2.42
97	97G1	" "	" "	+32° 43.16'	-117° 28.63'	524	1.66
97	97G2	" "	" "	+32° 43.15'	-117° 28.53'	555	1.09
98	98G	" "	San Diego Trough	+32° 37.53'	-117° 33.99'	1193	2.20
99	99G	" "	" "	+32° 37.44'	-117° 33.51'	1180	2.0
100	100G	" "	Coronado Bank	+32° 38.46'	-117° 26.55'	165	c.c. only
101	101G	" "	" "	+32° 39.04'	-117° 25.32'	167	0.29
102	102D2	Dart Core	" "	+32° 38.29'	-117° 25.75'	145	0.57
103	103G	Gravity Core	" "	+32° 39.45'	-117° 24.72'	355	0.95
104	104G1	" "	" "	+32° 38.90'	-117° 24.87'	303	0.25
104	104G2	" "	" "	+32° 38.65'	-117° 24.67'	350	0.29
104	104G3	" "	" "	+32° 38.43'	-117° 24.54'	332	0.70
105	105G	" "	" "	+32° 36.96'	-117° 22.70'	242	1.50
106	106G	" "	" "	+32° 36.75'	-117° 23.28'	256	1.03
107	107D1	Dart Core	" "	+32° 36.59'	-117° 23.77'	140	0.35

St a	Sample Number	Sample Type	Location	Latitude	Longitude	Water Depth(m)	Sample Length(m)
108	108G	Gravity Core	San Diego Shelf	+32° 37.57'	-117° 20.69'	162	0.71
109	109G	" "	"	+32° 37.36'	-117° 21.42'	192	1.99
110	110G	" "	"	+32° 43.55'	-117° 19.58'	080	0.76
111	111G	" "	"	+32° 43.16'	-117° 20.00'	089	0.20
112	112G	" "	Del Mar Shelf	+32° 56.98'	-117° 19.26'	293	1.48
113	113G	" "	"	+32° 56.82'	-117° 19.39'	250	1.13
114	114G	" "	"	+32° 57.09'	-117° 19.08'	193	1.83
115	115G	" "	"	+32° 57.21'	-117° 18.80'	081	0.40
116	116G	" "	"	+32° 57.08'	-117° 19.02'	180	1.79
117	117G	" "	"	+32° 57.10'	-117° 19.06'	186	1.56
118	118G	" "	Carlsbad Shelf & Slope	+33° 05.13'	-117° 22.79'	276	1.50
119	119G1	" "	"	+33° 05.03'	-117° 22.95'	211	0.45
119	119G2	" "	"	+33° 05.00'	-117° 23.03'	207	c.c.only
120	120G	" "	"	+33° 00.85'	-117° 26.04'	595	1.50
121	121G	" "	"	+33° 00.54'	-117° 26.19'	666	1.96